
CHAPTER

22

**PROPERTIES OF CONTINUOUS
FIBER-REINFORCED CERAMIC
MATRIX COMPOSITES FOR GAS
TURBINE APPLICATIONS**

Edgar Lara-Curzio

Metals & Ceramics Division, Oak Ridge National Laboratory, Oak Ridge, Tennessee, USA

INTRODUCTION

Improvements in the efficiency of gas turbine engines have been achieved by increases in turbine inlet gas temperature (TIT) through remarkable progress in component cooling and engine materials [1]. Because metallic materials currently used in the hot section of engines operate at 90% of their incipient melting temperatures, further improvements in efficiency will only be possible through the use of ceramic materials. It has been projected that fully optimized gas turbine engines incorporating ceramics would have significant increases in thermal efficiency and output power compared to all metal-engines with air-cooled components. Furthermore, such new gas turbine designs would offer increased performance, improved control of emissions and the potential for longer service lives.

Ceramics encompass all solids that are neither organic nor metallic. Compared with metals, ceramics have superior wear resistance, high temperature strength, and chemical stability. They also generally have lower thermal conductivity, thermal expansion, and lower toughness. The lack of toughness causes them to fail catastrophically, which is an undesirable trait if they are to be used in gas turbines engines. Several approaches have been followed to improve the toughness of ceramics. These include microstructural design and toughening by the addition of dispersed ceramic particulates, whiskers, or fibers to form ceramic matrix composites (CMCs). Among the various types of CMCs, Continuous Fiber-reinforced Ceramic Matrix Composites (CFCCs) are particularly attractive for gas turbine engine applications because of their ability to alleviate elastic stress concentrations at holes and notches by redistributing stresses through various inelastic deformation mechanisms [2].

As with all composite materials, the thermomechanical behavior and physical properties of CFCCs are determined by the properties of their constituents (i.e., fiber, fiber coating, matrix, matrix coating and their interfaces), by the architecture of the reinforcing fibers, and by a number of micromechanical mechanisms that include matrix cracking and fiber debonding and sliding to bridge the wake of advancing cracks in the matrix. The most widely used fiber architectures include woven fabrics (plain and satin weaves) but CFCCs also have been densified with simpler (e.g., stacking unidirectional layers) or more complex (e.g., 2-D polar, 2.5-D and 3-D) fiber architectures. Because most of the CFCCs that have been used for gas turbine engine applications are reinforced with 2-D continuous fiber architectures, the bulk of the data presented in this chapter corresponds to the properties of those materials.

Although most of the data available for CFCCs intended for gas turbine applications is for composites reinforced with SiC-based fibers and SiC matrices, data have been reported for CFCCs reinforced with carbon and oxide fibers (e.g. alumina, mullite) and CFCCs with carbon, glass-ceramic and oxide matrices. By far, carbon has been the most widely used fiber coating for CFCCs. The role of the fiber coating in CFCCs is to protect fibers during matrix synthesis and to facilitate fiber debonding and fiber sliding in the wake of advancing cracks in the matrix. However, the lack of oxidation resistance of carbon at temperatures above 300°C has prompted extensive work on the development of oxidation-resistant fiber coatings for CFCCs. Some of these fiber coatings include BN, Si-doped BN, multilayered coatings of C and SiC, pseudo-porous SiC and oxide fiber coatings [3].

Silicon carbide-based CFCCs are by far the most mature among CFCC systems with non-oxide matrices. This has been the result of more than 30 years of continuous R&D of SiC-based fibers and matrices. However, the lack of long-term environmental stability of SiC-matrix CFCCs in combustion-related environments (high-temperature, high-pressure, high-concentration of water vapor) has prompted the development of protective coatings (environmental barrier coatings or EBCs) and growing interest in all-oxide CFCCs because of the intrinsic stability of the latter in oxidizing environments. In contrast to the mechanisms responsible for providing damage tolerance in SiC-based CFCCs, damage tolerance in oxide/oxide CFCCs without fiber coatings is achieved by a network of fine pores in the matrix [4]. The mechanical characteristics of these materials are similar to those of carbon/carbon CFCCs but with superior oxidation resistance. Tensile fracture of all-oxide CFCCs occurs with substantial fiber pull-out although it doesn't conform to the classical model of individual fibers debonding and sliding out of their mating sockets in the matrix. Instead it involves fragmentation of the matrix and rearrangement of the surrounding matrix particles as the fibers slide [4]. However, the long-term thermal stability between the fibers and matrix in interphaseless all-oxide CFCCs remains a subject of concern, which has prompted significant efforts towards the development of fiber coatings for these CFCCs [5]. The use of all-oxide CFCCs is currently limited by the microstructural stability of the reinforcing fibers, which are less resistant to creep deformation than SiC fibers. Oxide fibers are prone to grain growth at high-temperatures, which results in loss of strength with time [6–10]. Although some single-crystal oxide fibers (e.g.—sapphire, YAG) possess good creep and stress-rupture resistance [6], their large diameter and high cost will limit their use to special applications with simple geometries.

Various routes have been established for the synthesis of CFCCs [11,12]. In the case of silicon carbide matrix composites, most systems are synthesized by chemical vapor infiltration (CVI), by the continuous impregnation and pyrolysis of polymer precursors (PIP) or by the infiltration and reaction of molten metals and alloys (MI). In the case of oxide-oxide composites, most systems are synthesized by sol-gel, powder processing and directed metal oxidation.

Most of the initial work to develop CFCCs for gas turbine engine applications took place in the UK during the 1950s and 1960s with the development of glass and glass ceramic matrix composites reinforced with carbon and silicon carbide fibers [13–18].

In subsequent years several programs were implemented in the U.S., Europe and Japan, to further research and develop CFCCs for gas turbine applications. In the U.S., these programs include, for example, U.S. Department of Defense Programs to develop fiber-reinforced glass and glass-ceramic matrix composites [19]; the U.S. Department of Energy's Continuous Fiber-Reinforced Ceramic Matrix Composites Program

to address the long-term R&D priorities identified by industry as the key to the development of CFCCs for Industrial Applications, including stationary gas turbine engines [20]; the U. S. Department of Energy's Ceramic Stationary Gas Turbine Development Program to improve the performance of stationary gas turbines in cogeneration through the selective replacement (retrofit) of metallic hot section parts with uncooled ceramic components [21]; NASA's Enabling Propulsion Materials (EPM) Program, to develop a 1200°C combustor liner for high-speed civil transport [22]; the Ultra Efficient Energy Technologies (UEET) Program to develop SiC/SiC CFCCs for hot-section gas turbine engine components [23]; the Integrated High Performance Turbine Engine Technology (IHPTET) Program, which is a joint DoD/NASA/Industry effort to develop advanced engine technologies, including C/SiC turbine rotor and nozzles, and SiC/SiC inter-turbine transition ducts [24]; and the NASA Advanced High Temperature Engine Materials Technology (HITEMP) Program [25,26].

SEP (Société Européenne de Propulsion) and DRET (Direction de Recherches, Etudes et Techniques), the French military research agency, sponsored some of the first programs to research and develop CFCCs for use in gas turbines in France, in particular to fabricate afterburner components (exhaust cone and flame-holder) and exhaust nozzles for the SNECMA M88 engine [27,28]. In The Netherlands a consortium sponsored by the Agency for Energy and the Environment worked towards the development of CFCCs for nozzles and a small turbine wheel for the Dutch OPRA and AMT turbines [29,30]. In Europe, the Commission of the European Communities sponsored the Human Capital and Mobility Program to develop and characterize carbon- and SiC-based CFCCs for advanced gas turbines [31].

In Japan, a consortium of government agencies and private organizations made extensive use of monolithic ceramics, CMCs and CFCCs to develop a 100 kW gas turbine with thermal efficiency over 40% at a turbine inlet temperature of 1350°C as part of the Automotive Ceramic Gas Turbine (CGT) Development Project [32]. The Research Institute for Advanced Materials Gas Generator, which is a joint effort by Japan's Key Technology Center and 14 Japanese corporations, implemented R&D programs to develop and use CFCCs for the manufacture of gas turbine engine stationary and rotating components [33,34] and more recently the CREST-ACE Program to research and develop SiC-based CFCCs with sound life cycles for advanced energy systems [35].

In the next section, examples of gas turbine engine components manufactured with CFCCs are discussed. This is followed by a compilation of CFCC properties that are relevant to gas turbine engine applications. Directions for future developments are also discussed.

COMPONENTS

Combustor Liners

The most common pollutants generated by gas turbines include NO_x, CO and unburned hydrocarbons. Burning the fuel after premixing it with excess air is particularly effective at reducing NO_x. Excess air in the reaction zone of the combustor acts as a heat sink that lowers the flame temperature to the point where no NO_x is produced in the combustor. If the combustion liner is film cooled, as is necessary when using conventional superalloys, a good fraction of combustor air is not available for premixing with the fuel. Consequently it is impossible to operate the combustor lean enough to remain below the NO_x formation threshold [1,36]. Combustion liners constitute the most widely explored application of CFCCs for gas turbine engines components because CFCCs have the potential of withstanding the temperature of the hot gas in the reaction zone without film air cooling. Furthermore, in this application mechanical loads are minimal and stresses arise mostly from thermal gradients. Using the available air for lean premixing, rather than for film air cooling, results in a reduction of NO_x emissions. CO and unburned hydrocarbon emissions would also be reduced because the hot surface of a CFCC combustor liner could be operated at a temperature high enough to ensure that the fuel oxidation reactions were not quenched at the combustor walls.

In the U.S., the Department of Energy has sponsored various programs (e.g. the Ceramic Stationary Gas Turbine Development Program, the Continuous Fiber Ceramic Composites Program, and the Advanced Turbine Systems Program) to develop and demonstrate the use of CFCC combustor liners [20–21,37–38]. For example, as part of the Ceramic Stationary Gas Turbine (CSGT) Development Program, Solar Turbines Inc., has evaluated inner and outer SiC-based CFCC combustor liners in an industrial gas turbine engine with nominal power output of 4 MWe [21,39]. To date SiC-based CFCC combustor liners have accumulated more than 55,000 hours of engine operation. These engine runs were preceded by screening tests in which CG-NicalonTM/SiC, Al₂O₃/Al₂O₃ and CG-NicalonTM/Al₂O₃ subscale combustor liners were evaluated in a burner rig that simulates actual engine temperatures and pressures [40]. These screening tests showed that CG-NicalonTM/SiC exhibited the best performance of the liners evaluated. Figure 22.1 shows pictures of Hi-NicalonTM/CVI-SiC combustor liners for a Solar Centaur 50S gas turbine engine and a Hi-NicalonTM/MI-SiC combustor liner for an industrial-grade gas turbine engine. Several CFCC combustor liners have also been evaluated for military aeroengines [41].

In Japan, several programs have been focused on the development, fabrication and demonstration of SiC/SiC and C/SiC CFCC combustor liners for gas turbines used in the Super/Hypersonic Transport Propulsion System (HYPR), for the Advanced Material Gas-Generator (AMG), for a 100 kW automotive ceramic gas turbine and for helicopter turboshaft engines [32,34,42–44].

Programs in both Europe and the US have also been focused on using all-oxide CFCCs to manufacture combustor liners as an alternative to SiC-based CFCCs. Although all-oxide CFCCs have the potential of exhibiting improved stability in high-temperature oxidizing environments, they possess lower thermal conductivity than their SiC-based counterparts, which could result in higher thermal gradients and stresses. Also, the lower resistance of oxide fibers to creep deformation and the loss of fiber strength with time is a potential limitation of these materials. In Europe the four-year long program “Novel Oxide Ceramic Composites (NOCC)” was implemented to develop processing routes to fabricate an all-oxide CFCC combustor liner and to demonstrate it in a combustor rig at conditions representative of a gas turbine engine [45–48]. The all-oxide CFCC, which was synthesized by tape casting followed by hot pressing, consisted of single crystal alumina monofilaments, an alumina matrix and a zirconia fiber coating. Figure 22.2 shows a photograph of the all-oxide combustor tiles produced during this program. A tile was successfully tested in a rig at temperatures above 1260°C, but the major issues that remain to be addressed included high cost, delamination dur-

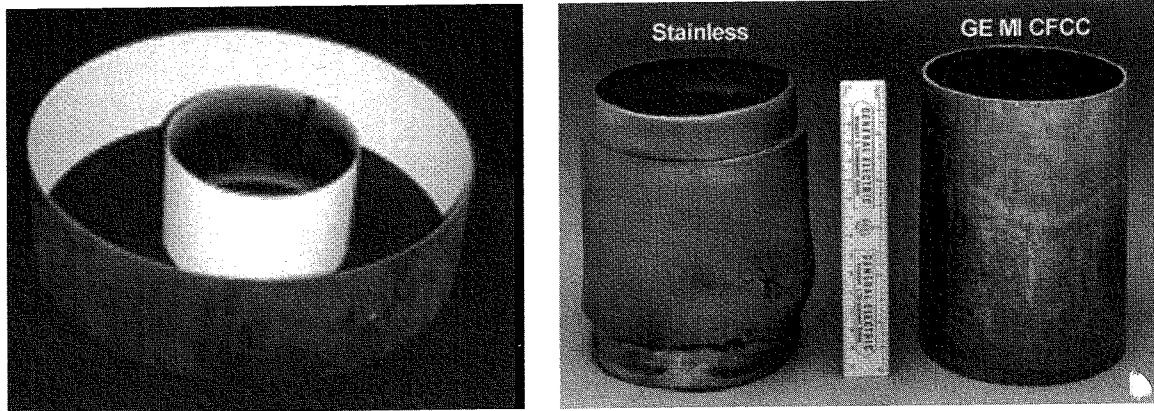


Figure 22.1 (a) Set of EBC Coated Liners Tested by Solar for 13,937 hrs—Inner Liner—Hi-NicalonTM/MI-SiC; Outer Liner—Hi-NicalonTM/SiC E-CVI (Reprinted from ref. [39]). **(b)** Hi-NicalonTM/MI-SiC CFCC Combustor Liner and Stainless Steel Counterpart (Reprinted from ref. [38]).

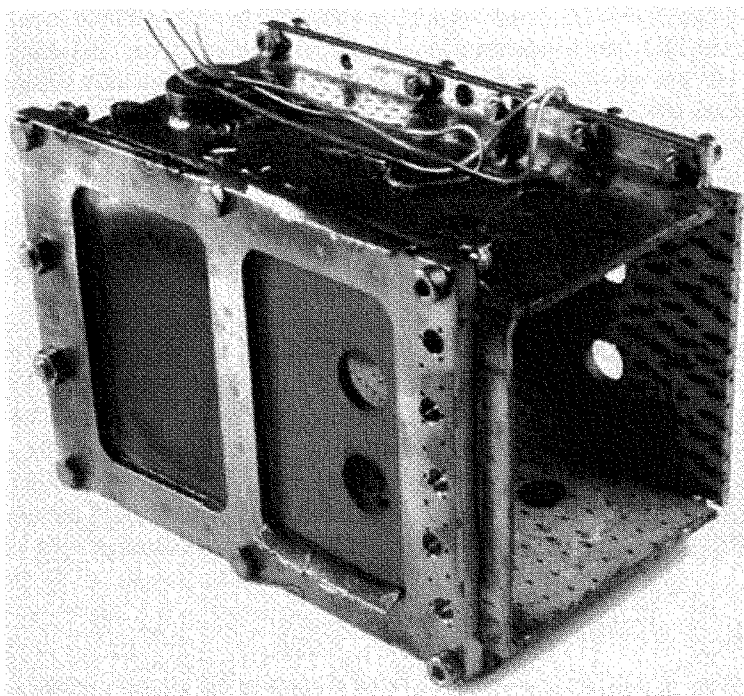


Figure 22.2 Combustor Can with All-Oxide CFCC Tiles
(Reprinted with permission from ref. [46])

ing manufacture, and consistency in properties. Other programs in Europe have also investigated the potential use of C/C, SiC/SiC, and C/SiC CFCC combustor liners [49].

Flaps and Seals

Another popular application of CFCCs in gas turbine engines is for flaps and seals [50–54]. Several CFCC systems (e.g.—CG-NicalonTM/Carbon, CG-NicalonTM/SiNCO, CG-NicalonTM/Al₂O₃ and NextelTM 610/aluminosilicate) have been evaluated and their use has been demonstrated for these applications. While some of these CFCCs exhibited through-the-thickness cracking or excessive wear after screening tests, CG-NicalonTM/SiNCO and CG-NicalonTM/C were able to withstand successfully the conditions of this application [51].

Rotors and Blades

CFCCs have also been considered for the manufacture of rotating parts in gas turbine engines. In contrast to combustor liners or flaps, where stresses arise from thermal gradients and wear, in rotating parts the magnitude of stresses generated during service is significantly higher and proportional to the rotational speed. To optimize the resistance of CFCCs to stresses associated with high rotational speeds, special fiber architectures have been developed, which align the fibers along the direction of maximum stress (e.g.—fabrics with 2-D polar weaves for example). Cold spinning tests have shown that CFCCs are capable of withstanding the stresses associated with rotating gas turbine engine components and several prototypes of rotating disks have been fabricated using carbon and CG-NicalonTM fibers [55–60]. For example, C/C,

C/PIP-SiC and Hi-NicalonTM/PIP-SiC rotors have been subjected to cold spinning tests and foreign object impact at speeds over 600 m/s, which correspond to the maximum speed of the blade tips [61]. C/SiC CFCC turbine rotors for the 100 kW automotive ceramic gas turbine project in Japan have withstood 90,000 rpm in cold spin tests [32]. Although the ultimate strength of many CFCCs is higher than the peak stress in these applications, the propensity of non-oxide CFCCs to environmental attack at stresses larger than the matrix cracking stress in combustion environments, and the expectancy of tens of thousands of hours of service life most likely will prevent their use for this application.

Shrouds

Components in the first stage of gas turbine engines (e.g.—shrouds) are exposed to some of the highest gas temperatures in the engine. Currently shrouds consist of coated nickel-based superalloys and the maximum capability of these materials limits the shroud temperature to below 1000°C, therefore requiring the use of cooling air. This results in substantial penalty in efficiency. CFCCs may satisfy the environmental and mechanical requirements, while at the same time substantially reducing the need for cooling air, resulting thus in improved engine efficiency. Programs in the U.S. and Japan have demonstrated the use of CFCCs for the fabrication of shrouds [32,62]. Figure 22.3 shows a SiC/Mi-SiC shroud compared to its metallic counterpart.

TEST METHODS

In many instances the design and manufacture of CFCC components for gas turbine engines has followed the process illustrated in Figure 22.4. This process involves the use of standardized test methods to evaluate the physical and mechanical properties of CFCCs; the assembly of data bases with data generated through the

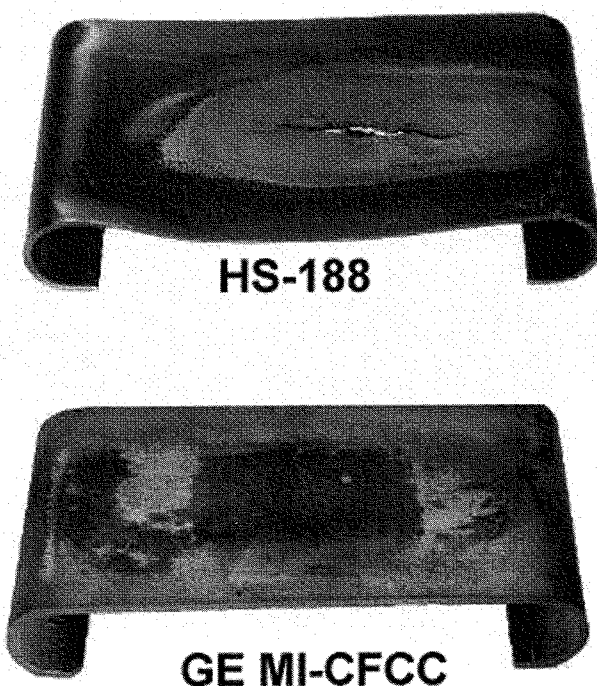


Figure 22.3 MI-CFCC Shroud and Metallic Counterpart (Adapted from ref. [62])

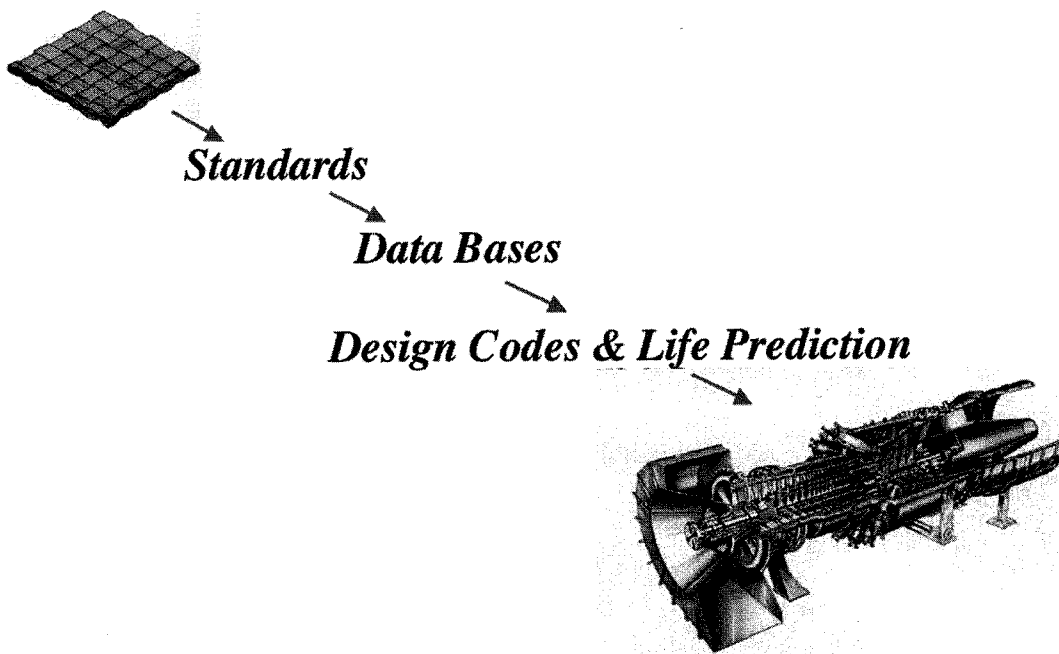


Figure 22.4 Process for the Design and Implementation of CFCCs in Gas Turbine Applications

use of full-consensus standardized test methods; and design codes. These design methodologies address the statistical nature of the strength of the CFCC constituents and are aimed at predicting their durability and reliability. Design methodologies usually start with the determination of stresses and strains through finite-element stress analyses. This requires knowledge of the properties of candidate materials for that design, which after being obtained through standardized test methods, would be available in data bases. Issues associated with fatigue, stress-rupture and environmental effects on mechanical and physical properties then can be addressed. In the U.S. an effort is currently under way to develop a design handbook for using CFCCs in gas turbines and industrial applications, as part of the DOD MILITARY HANDBOOK 17. The design methodologies contained therein depend strongly on the availability of data obtained according to full-consensus standardized test methods along with results from the evaluation of materials under special simulated or actual conditions of temperature and environment. Similar efforts are undergoing in Europe and Japan [63].

In the United States, the American Society for Testing and Materials (ASTM) has spearheaded the widespread introduction of standard test methods for advanced ceramics and ceramic composites [64,65]. In Europe, technical committee 184 of the Committee for European Normalization (CEN TC-184) is the organization responsible for the development of full-consensus test standards for CFCCs. In Japan, the Petroleum Energy Center has been one of the organizations responsible for sponsoring the preparation of several industry-accepted test standards for CFCCs [66]. Recently, international harmonization activities have resulted in the drafting of four international standards for CFCCs (tension, compression, in-plane shear and interlaminar shear) within the jurisdiction of technical committee 206 on Advanced Technical Ceramics of the International Standards Organization (ISO TC-206) [65]. Work is still needed to standardize the nomenclature related to CFCC and data reporting practices. For example, general references to "SiC/SiC composites" are meaningless considering the many forms and types of SiC-based fibers, fiber coatings, fiber architectures, and forms of SiC matrices that are currently available. Additional information on standardization of CFCCs can be found in chapter 24 of this volume.

In general, each gas turbine engine component has different material requirements. For example, combustor liners require materials with good thermal conductivity, good corrosion resistance and tolerance to foreign object impact. Materials for rotating components must have high tensile strength, high creep and fatigue resistance, whereas materials for nozzle flaps and petals must be resistant to erosion, corrosion and acoustic fatigue. In the following sections the properties of candidate CFCC materials for gas turbine applications are reviewed. Experimental results are presented for elastic constants, tensile and shear strength in various material planes, fracture resistance, performance-related behavior (e.g., resistance to mechanical fatigue, creep, stress-rupture, and thermal shock) thermal and physical properties (e.g., thermal conductivity and thermal expansion). Environmental effects (e.g., oxidation, corrosion) on mechanical performance and physical and mechanical properties of these materials are also reviewed.

MECHANICAL PROPERTIES

Figure 22.5 shows a typical tensile stress-strain curve for a 2-D CG-NicalonTM/PIP-SiNCO CFCC with a 0.1- μm thick fiber coating of BN and a fiber volume fraction of 40%. Also included in the plot is a record of the acoustic emissions generated by the material upon successive loading/unloading and reloading cycles to increasingly larger levels of stress. This stress-strain curve in Figure 22.5 exhibits well-defined regimes associated with: linear elastic behavior up to the proportional limit stress, σ_{pl} , and non-linear inelastic behavior for larger stresses. It can also be observed that the Felicity ratio, which may be used as a measure of damage and is defined as the ratio between the value of tensile stress at which acoustic emissions start upon reloading, divided by previous maximum tensile stress, decreases with increasing peak stress [67]. The hysteresis that occurs during unloading-reloading cycles relates to the magnitude of the interfacial shear stress. The three mechanisms responsible for the non-linear stress-strain behavior exhibited by many CFCCs are [68]: (1) matrix cracking; (2) changes in the residual stress distribution as a result of matrix

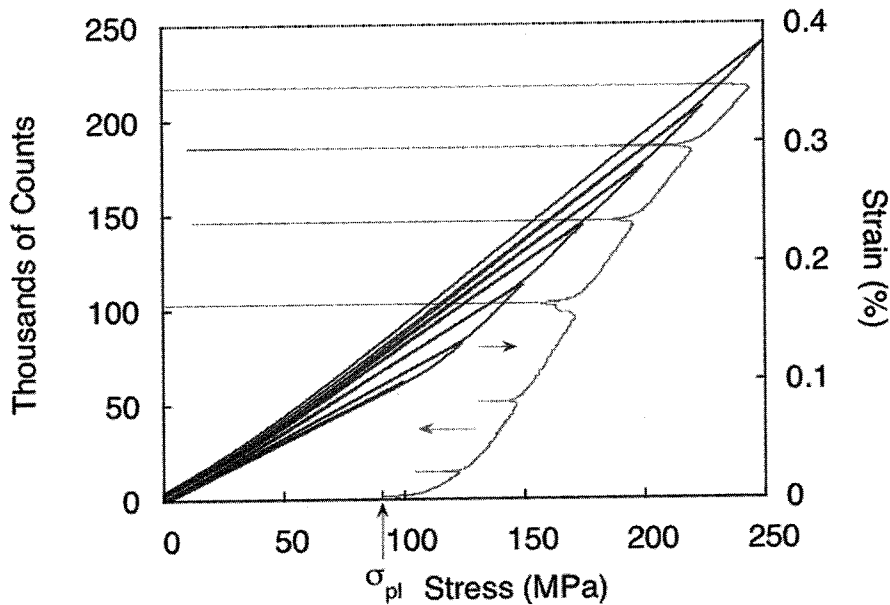


Figure 22.5 Tensile Stress-Strain Curve for CG-NicalonTM/BN/Si-N-C-O CFCC Obtained After Multiple Loading-Unloading Cycles. Also Enclosed are Acoustic Emissions Recorded During the Test. The Onset of Acoustic Emissions Indicates the Onset of Cracking in the Matrix.

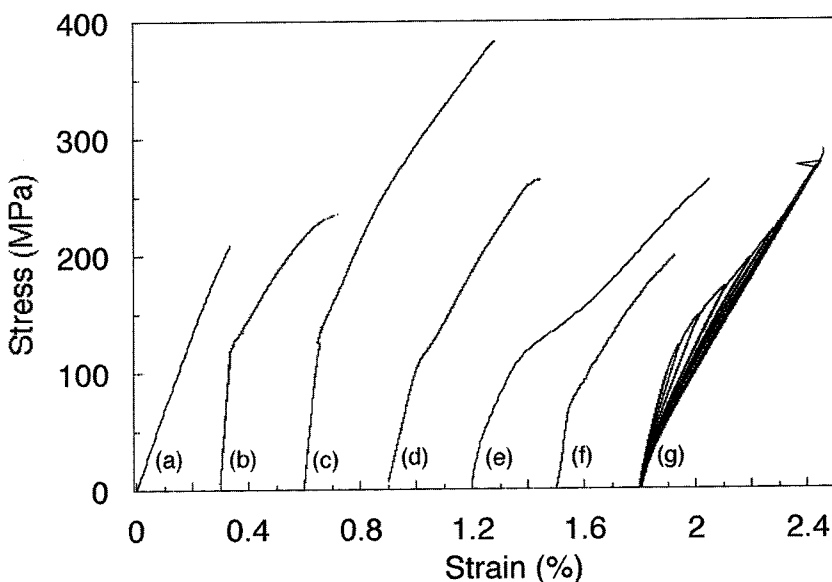


Figure 22.6 Typical Tensile Stress-Strain Curves of CFCCs. (a) 8-Harness Satin Weave Nextel 610/Sol-Gel SiO₂Al₂O₃ (b) 8-Harness Satin Weave Hi-Nicalon™/CVI SiC with Multilayered C/SiC Interfacial Coating (c) 5-Harness Satin Weave Hi-Nicalon™/CVI SiC with BN Interfacial Coating (d) 8-Harness Satin Weave CG-Nicalon™/ Polymer Impregnation and Pyrolysis Si-N-C-O with BN Interfacial Coating (e) 5-Harness Satin Weave CG-Nicalon™/ Directed Metal Oxidation Al₂O₃ with Dual BN/SiC Interfacial Coating (f) Plain Weave CG-Nicalon™/CVI SiC with Carbon Interfacial Coating (g) Plain Weave CG-Nicalon™/BMAS Glass-Ceramic with Dual BN-SiC Interfacial Coating.

cracking; (3) frictional dissipation that occurs at the fiber/matrix interfaces and that is dominated by the fiber coating, the fiber morphology and the topography of the fiber's surface. By varying the magnitude of the interfacial shear stress, the prevalent damage mechanism and the resultant non-linear stress-strain behavior can be dramatically modified. Figures 22.6 and 22.7 show a collection of tensile stress-strain curves for various types of CFCCs. Note that the shape of the curves is affected by the type of fiber, matrix and fiber architecture. The stress-strain curves obtained from the tensile evaluation of 0/90 oxide-oxide composites exhibit very slight nonlinearity that increases with increasing stress. In contrast, the stress-strain curves obtained from the evaluation of all-oxide composites with $\pm 45^\circ$ fiber architecture exhibit lower elastic modulus and ultimate strength, but greater capacity to inelastic straining (Figure 22.7).

Elastic Properties

Various techniques have been used to determine the elastic properties of CFCCs. These include the recording of stresses and strains within the elastic range during mechanical testing, and ultrasonic and small-amplitude vibration methods. Ultrasonic techniques have the advantage of being non-destructive and by aligning a particular direction of the material with the direction of propagation of the ultrasonic pulse, the elastic property of the material in that direction can be obtained. Ultrasonic techniques can be applied at elevated temperatures and therefore can be used to detect changes that may result from reactions between the material and the environment. For example, when CFCCs with SiC-based fibers and carbonaceous fiber coatings are exposed to air at elevated temperatures, the fiber coating will oxidize, resulting in loss of stiffness. This initial loss in stiffness is followed by an increase in stiffness as a result of the formation

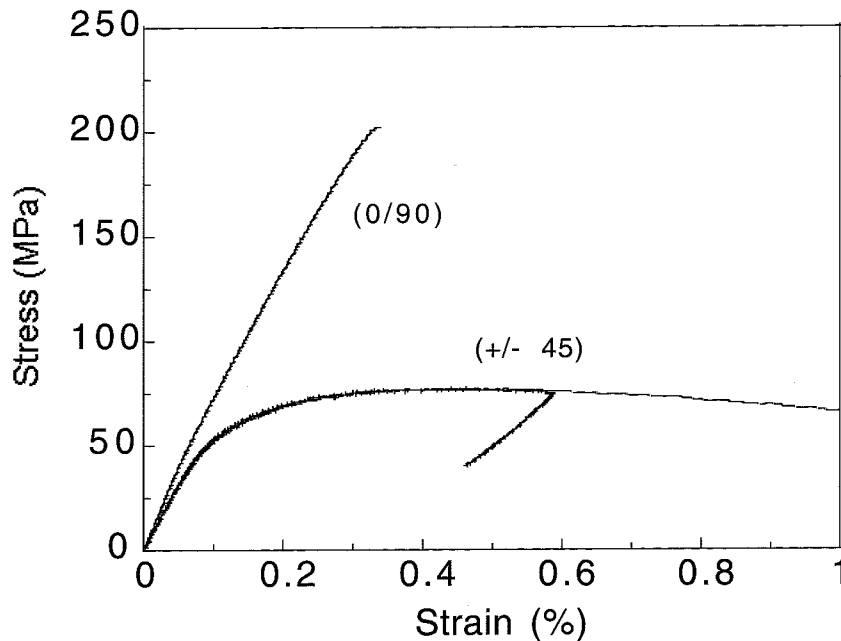


Figure 22.7 Tensile Stress-Strain Curves for Nextel™ 720/AS with (0/90) or ($\pm 45^\circ$) Fiber Orientation. Two Curves are Presented for the Latter to Illustrate the Reproducibility of Response

of silica on the surface of the fiber, and the filling of the gap previously occupied by the fiber coating with silica [69, 70]. Table 22.1 lists the elastic properties of several CFCCs along with the technique used for their determination.

In-plane Tensile Behavior

In 1999 a round-robin testing program was completed in the U.S. to determine the precision of ASTM test standard C1275 "Standard Test Method for Monotonic Tensile Strength Testing of Continuous Fiber-Reinforced Advanced Ceramics with Solid Rectangular Cross-Section Specimens at Ambient Temperatures" [82]. From this study coefficients of variation for repeatability and reproducibility were obtained for elastic modulus, proportional limit stress, ultimate tensile strength and strain at fracture of CG-Nicalon™/PIP SiNCO. However, no statement of bias was given because no acceptable reference standard material exists at this time. The elastic properties obtained for this CFCC as part of this study are listed in Table 22.1. Figure 22.8 shows a summary of the tensile strength results obtained by the nine laboratories that participated in the study, with each laboratory testing ten tensile specimens. The plot shows the great mean value and one standard deviation with respect to this value.

Limited studies have been carried out to assess the effect of specimen geometry, mode of loading (force versus displacement control), and rate of testing on the tensile strength and stress-strain behavior of CG-Nicalon™/CVI-SiC CFCCs [83]. It was found that for the range of values investigated, neither the test mode (displacement vs. force control) nor test rate (50 N/s vs. 500 N/s; 0.003 mm/s vs. 0.03 mm/s) had an effect on the proportional limit stress or ultimate tensile strength of the material. Although the geometry of the test specimens did not have an effect on the proportional limit stress, it was found that contoured tensile specimens with the smallest gauge length, for the range of values investigated, had the largest tensile strength. The in-plane tensile strength of CFCCs is size-dependent and this effect needs to be accounted for when designing components that are of different size from the standardized test specimens used for obtaining data [84,85].

TABLE 22.1 ELASTIC PROPERTIES OF CFCCs

Fiber	Matrix	V _f (%)	Fiber Architecture	Interface	Density (g/cm ³)	Porosity (%)	Technique	E (GPa)	G (GPa)	v	Ref
PAN-carbon	CVI-SiC	40	2D PW	1 μm PyC	2.0	10–15	ultrasonic	118 (4) 115 (12) 248 ¹ 130 ¹			[71] [72] [73]
CG-Nicalon™	CVI-SiC					14 30	ultrasonic				[74]
C	CVI-SiC	40	2D PW		2.0	10–15	tensile testing	140 (20°C) 145 (50°C) 135 (1000°C) 152 (1200°C)			
CG-Nicalon™	CVI-SiC + oxidation inhibitors	40	2D PW	PyC	2.58	9.7					[70]
CG-Nicalon™	CVI-SiC	33	8 plies 8HSW 0/90 8 plies 8HSW 0/90±45 8 plies 8 HSW ±45	PyC	2.54		tensile testing	240.6 (14.5) 219.3 (20) 182.7 (24.1)	75.8 (25.5) 92.4 (21.4) 101.4 (15.2)	0.19 (0.07) 0.19 (0.04) 0.20 (0.02)	[75]
CG-Nicalon™	CVI-SiC	41	5HSW with angle interlock between layers	0.5–1.0 PyC		10–15		237 (20°C) 238 (1200°C)			[76]
T300	CVI-SiC		0/90 0±45/90 ±45 0/90 0±45/90 ±45				tensile testing	60 (1550°C) 76			[77]
CG-Nicalon™	CVI-SiC			PyC			tensile testing	57 56 211 220			[77]
Tyranno™ Carbon Carbon	CVI-SiC CVI-SiC PIP-SiC porous alumina-mullite							210 190–210 90–100 60–80			[78]
Nextel™ 610		37–42	8HSW (0/90) 8HSW (±45) 8HSW (0/90)	—		23.7–24.9	tensile testing	96 50 78		.05 ² .55 ²	[79]
CG-Nicalon™ AS	PIP Si-N-C-O	42–48 48	0.5 μm BN 8HSW (0/90)	2.6			tensile testing	90.7 (3.7) 72 (980°C)	33 (2)	0.12 (0.01)	[80] [81]
CG-Nicalon™	CVI-SiC			—			ultrasonic	235 235	78.8 ³ 68.3 ⁴		[70]

Notes: 1-In-plane modulus; 2-V_{f1}; 3-G_{xz}; 4-G_{xy}, G_{yz}.

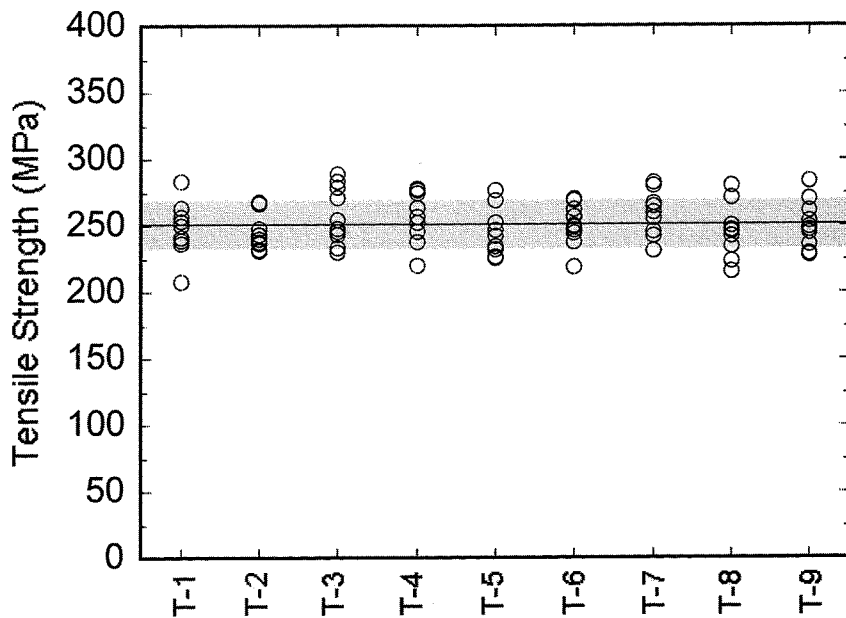


Figure 22.8 Summary of Tensile Strength Results for CG-Nicalon™/BN/SiNCO CFCC Obtained from Round-Robin Testing Program [80]

Figures 22.9 and 22.10 present tensile strength results for several continuous fiber-reinforced ceramic matrix composites as a function of temperature. Included in these graphs are data for composites reinforced with CG-Nicalon™ fibers, Hi-Nicalon™ fibers, T-300 graphite fibers, Nextel™ 610 and Nextel™ 720 fibers, Sumitomo® alumina-silica fibers, Bestfight™ carbon fibers, and Si-Ti-C-O Tyranno fibers. For composites with comparable fiber concentration and fiber architecture, CVI-SiC matrix composites reinforced with graphite fibers exhibit the highest tensile strength, and in inert environment, the best retention of strength at elevated temperatures. The effect of fiber stiffness (200 GPa for CG-Nicalon™ versus 270 GPa for Hi-Nicalon™) on the stiffness and on the magnitude of the proportional limit stress of CFCCs is evident in the tensile stress-strain curves presented in Figure 22.11 for SiNCO matrix CFCCs reinforced with CG-Nicalon™ and Hi-Nicalon™ fibers.

Even at room temperature, but particularly at elevated temperatures, the stress-strain behavior of CFCCs, including the magnitude of the matrix cracking stress and ultimate tensile strength, depend on the loading rate and loading mode [89–91]. At room temperature, the increase in the ultimate tensile strength of CFCCs can be attributed to an increase in interfacial shear stress with loading rate, whereas the load rate-dependence of the matrix cracking stress that has been observed for glass-ceramic matrix composites can be related to stress-corrosion cracking [90]. At high temperatures, as the loading rate increases—under force control—the ultimate tensile strength increases, but the opposite trend is observed when tensile tests are carried out under a constant displacement rate. These results suggest that the time-dependent deformation (e.g.—creep) and time-dependent redistribution of internal stresses in CFCCs [92] play a significant role. Figures 22.12–22.14 show results that illustrate the effect of loading rate on the ultimate tensile strength of CG-Nicalon™ fiber-reinforced CFCCs at high temperatures.

Transthickness Tensile Behavior

Because of the availability of ceramic fibers in tows and fabric form, most fiber preforms consist of stacked layers of woven fabric. As a consequence of the resulting laminated structure, 1-D and 2-D CFCCs exhibit large anisotropy between their in-plane and through-the-thickness physical and mechanical properties.

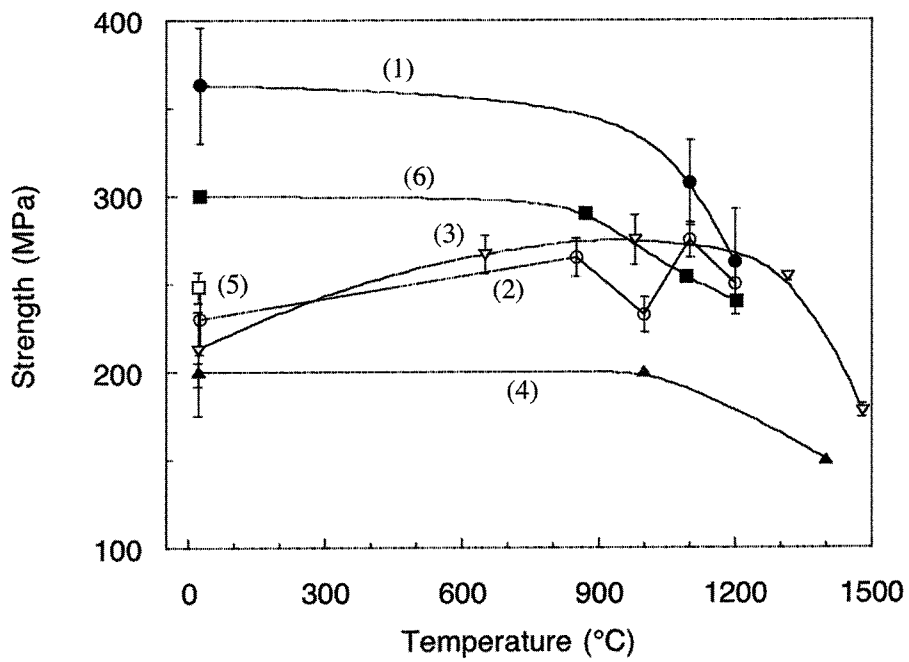


Figure 22.9 Tensile Strength Results for CFCCCs: (1) Hi-Nicalon™/C/CVI-SiC [77];
 (2) CG-Nicalon™/C/CVI-SiC [77]; (3) CG-Nicalon™/C/CVI-SiC [87];
 (4) CG-Nicalon™/C/CVI-SiC [86]; (5) CG-Nicalon™/C/CVI-SiC [75];
 (6) Hi-Nicalon™/BN/Mi-SiC [38].

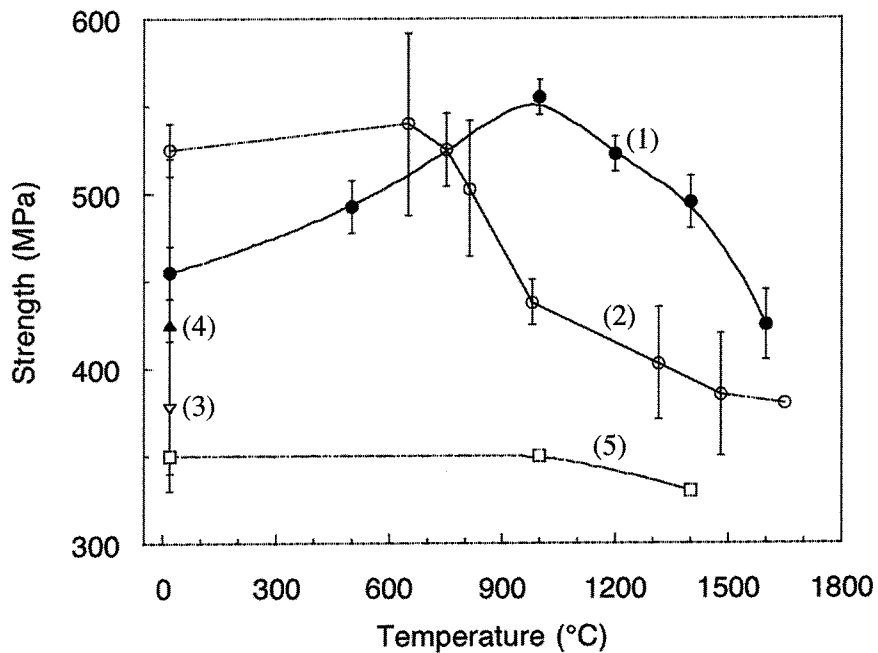


Figure 22.10 Tensile Strength Results for Carbon Fiber-Reinforced CVI-SiC. (1) [74]; (2) [88];
 (3) [87]; (4) [77]; (5) [86].

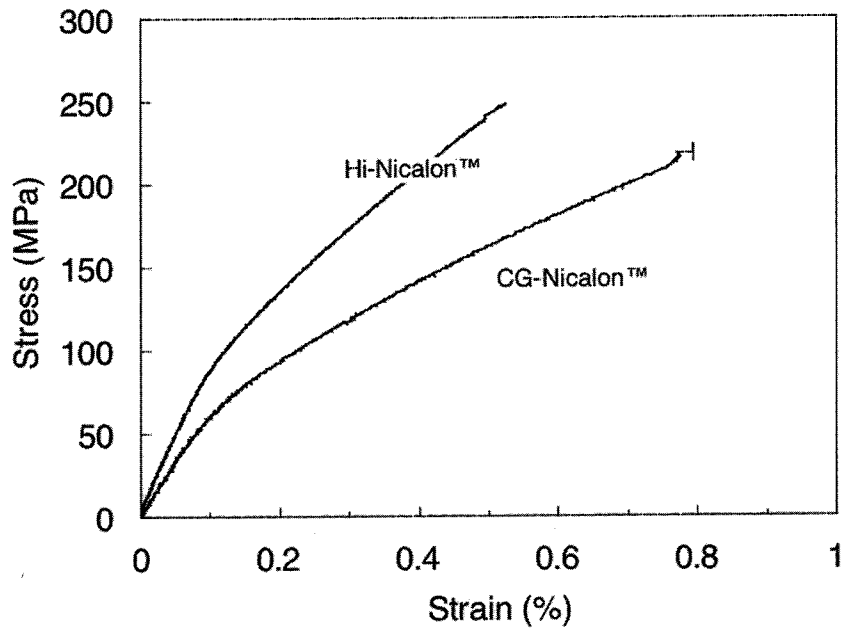


Figure 22.11 Effect of Fiber Type (CG-Nicalon™ versus Hi-Nicalon™) on the Monotonic Tensile Behavior of SiNCO Matrix CFCCs in Air at 1200°C

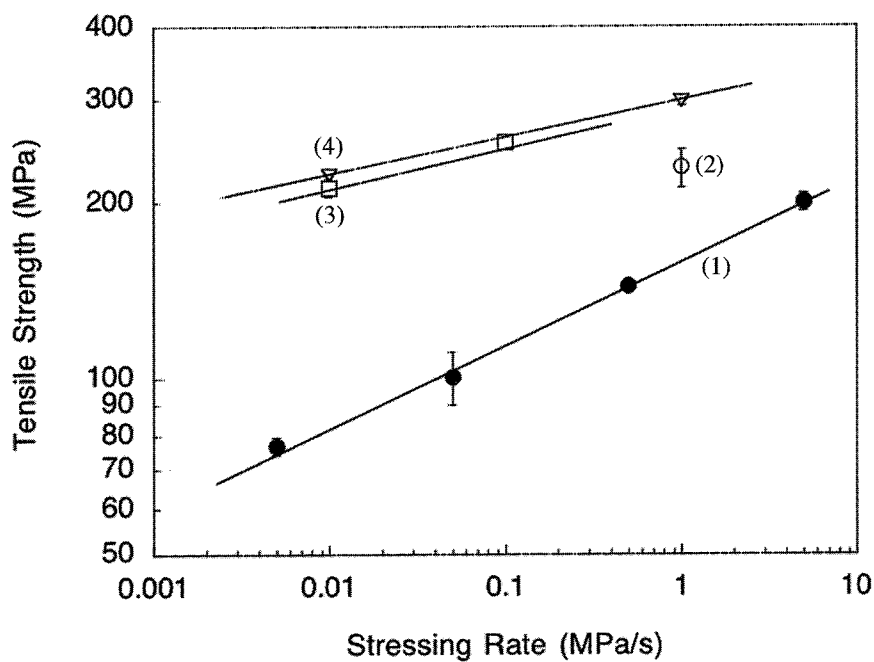


Figure 22.12 Effect of Loading Stress Rate and Temperature on the Tensile Strength of CFCCs: (1) CG-Nicalon™/C/CVI-SiC at 1200°C [89]. Open Symbols for CG-Nicalon™/BN/SiNCO [91]: (2) 23°C; (3) 1000°C; (4) 1200°C.

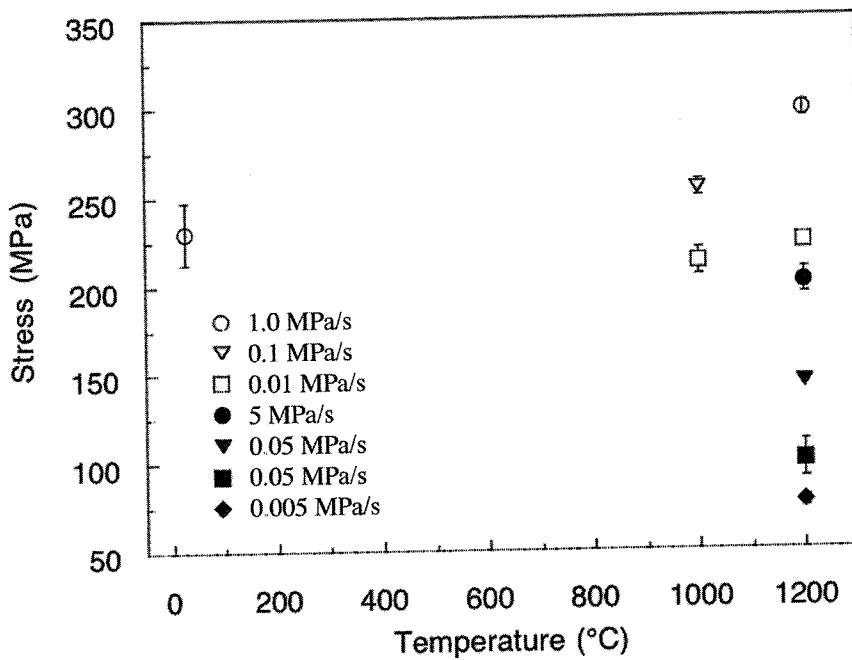


Figure 22.13 Effect of Loading Stress Rate and Temperature on the Tensile Strength of CFCCCs: Open Symbols for CG-NicalonTM/BN/SiNCO [91] and Close Symbols for CG-NicalonTM/C/CVI-SiC [89].

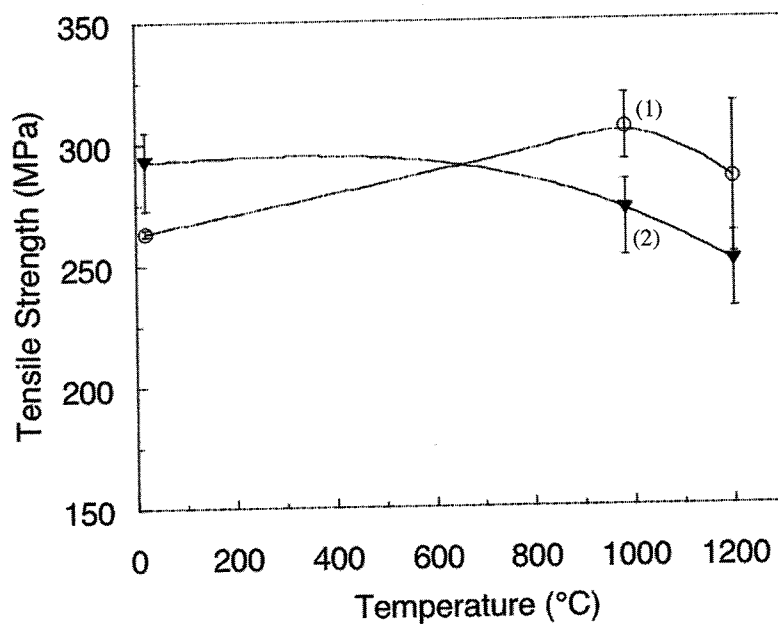


Figure 22.14 Effect of Temperature and Cross-Head Displacement Rate on the Tensile Strength of CG-NicalonTM/BN/SiNCO: (1) 25 µm/min and (2) 25 mm/min [91].

These differences have been accentuated due to efforts to optimize the in-plane tensile properties of CFCCCs, which have occurred at the expense of the interlaminar and transthickness properties. In laminated CFCCCs, the interlaminar shear and transthickness tensile modes of failure are dominated either by the properties of the matrix or by those of the fiber/matrix interface.

The optimization of the in-plane tensile properties of CFCCCs has been achieved through the use of “weak” fiber-matrix interfaces, which promote crack deflection and fiber debonding and sliding. However, these “weak” interfaces become the weakest link for the propagation of interlaminar and transthickness cracks when CFCCCs are subjected to tensile transthickness or shear loading. Figure 22.15 shows a series of stress-strain curves obtained from the transthickness tensile evaluation of unidirectional Hi-NicalonTM/CVI-SiC matrix composites with pyrocarbon fiber coating, in a direction normal to the fiber direction. The specimens were square in size (10 mm × 10 mm) and 2.3 mm thick. In this case, failure occurred along a plane that coincides with the fiber/matrix interface at a stress level lower than the matrix cracking stress associated with the onset of non-linear behavior during tensile loading. For this material, the ratio of the transthickness tensile strength to the tensile strength along the fiber direction was found to be 0.025, which illustrates the large degree of anisotropy in the strength of the material. Figure 22.16 summarizes transthickness tensile strength results for various CFCCCs obtained from the evaluation of circular test specimens of diameters between 15 and 25 mm, and square test specimens of size between 10 and 17 mm [93,94].

A new test method is currently being considered for standardization within ASTM’s sub-committee C28.07 on Ceramic Matrix Composites to determine the transthickness tensile strength of 1-D and 2-D CFCCCs. This test method is based on the diametral compression of circular specimens as illustrated in Figure 22.17. The advantage of this test method is that it can be carried out at elevated temperatures, in contrast to the currently accepted ASTM Test Method C1468-00 “Standard Test Method for Transthickness Tensile Strength of Continuous Fiber-Reinforced Advanced Ceramics at Ambient Temperature,” [95] which is limited by the properties of the adhesive used to transfer the load to the specimen.

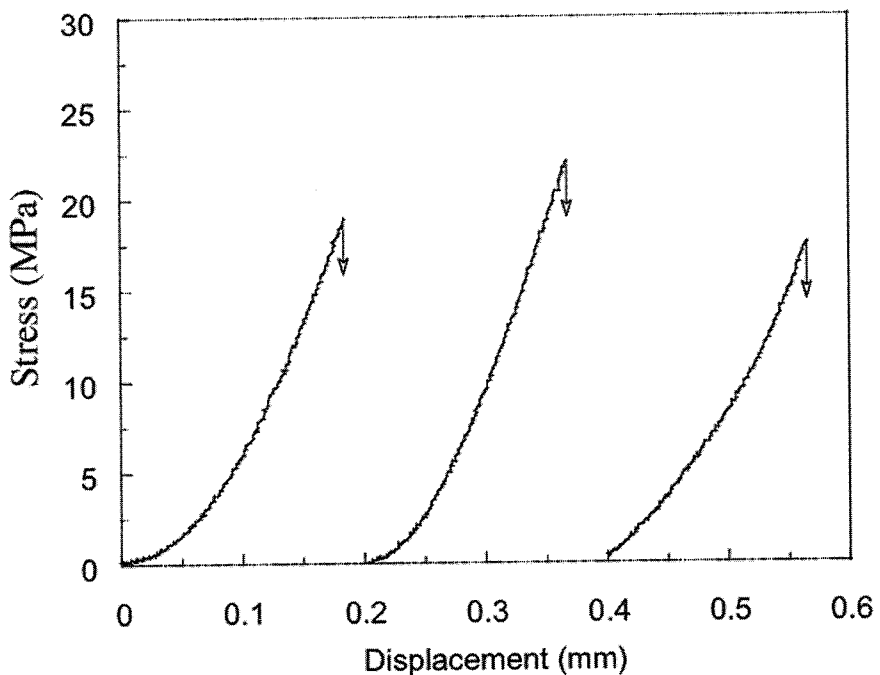


Figure 22.15 Typical Transthickness Stress versus Cross-Displacement Curve for 1-D Hi-NicalonTM/C/CVI-SiC [91]

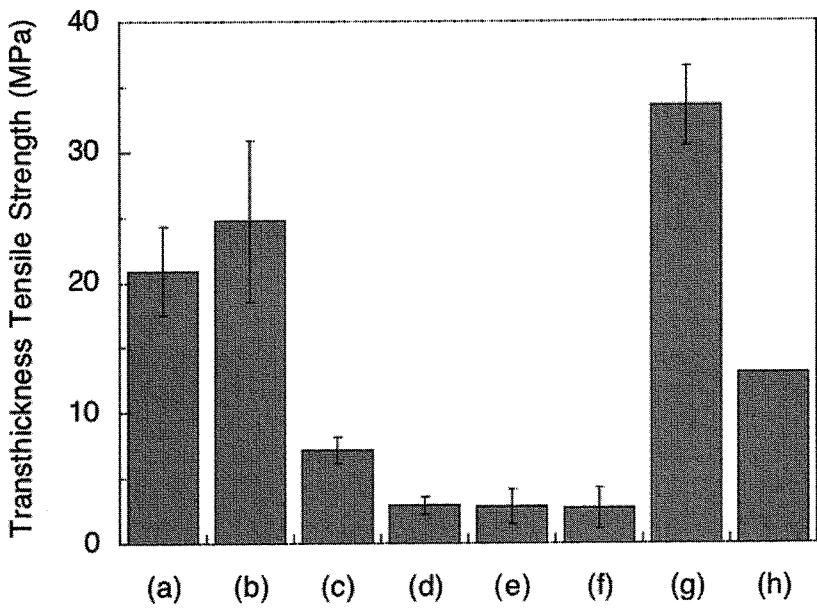


Figure 22.16 Transthickness Tensile Strength for 1-D and 2-D CFCCCs.
 (a) CG-NicalonTM/MAS-5; (b) CG-NicalonTM/BN/SiNCO; (c) NextelTM610/AS (GE);
 (d) NextelTM610/AS (3M); (e) NextelTM720/AS (GE); (f) NextelTM720/AS (COI);
 (g) SCS-6/Si₃N₄ (Unidirectional) [93]; and (h) CG-NicalonTM/C/CVI-SiC [94]

Shear Properties

The matrix cracking that occurs in 2-D CFCCCs when subjected to shear loading depends on the loading orientation and the properties of the matrix. For engineering applications, two dominant shear loading orientations are of interest: in-plane shear and interlaminar shear. For the case of interlaminar shear, matrix cracks evolve without significant interaction with the fibers. Conversely, for in-plane shear loading, matrix

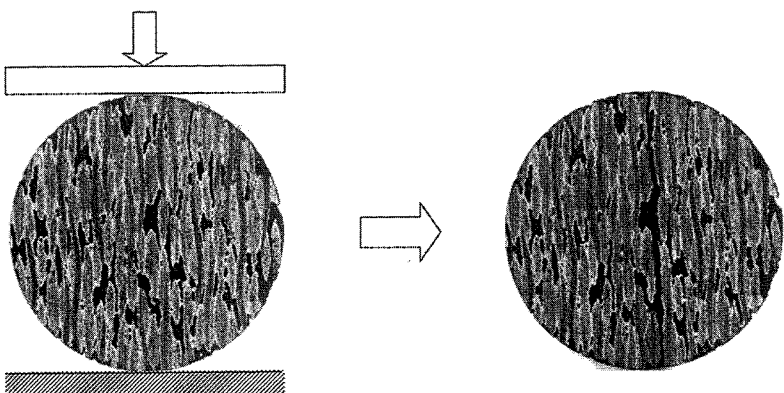


Figure 22.17 Schematic of Brazilian Test (Diametral Compression) to Determine the Transthickness Tensile Strength of CFCCCs. CG-NicalonTM/CVI-SiC CFCC Specimen
 (a) Before and (b) After Testing

cracks must interact with the fibers which impede crack development. Consequently, the in-plane shear strength always exceeds the interlaminar shear strength [68].

Analysis of experimental shear strength data indicates that the matrix has a major influence on the shear strength and the shear ductility of continuous fiber-reinforced ceramic matrix composites [68]. Among the various matrices available, CVI-SiC matrix composites exhibit some of the largest in-plane shear strengths among CFCCs. The in-plane shear strength of CFCCs can be ranked using a parameter given by

$$W = \sqrt{\frac{\Gamma_m}{rG}} \quad (1)$$

where Γ_m is the fracture energy of the matrix, G is the shear modulus of the matrix, and r is the fiber radius.

ASTM standard test method C1292 "Standard Test Method for Shear Strength of Continuous Fiber-Reinforced Ceramics at Room Temperature" was first introduced in 1996 to determine the in-plane and interlaminar shear strength of CFCCs based on the Iosipescu test method, and interlaminar shear strength by the compression of double-notched specimens. Figure 22.18 shows a photograph of an Iosipescu test fixture with specimens for in-plane and interlaminar shear strength determination, along with schematics of the Iosipescu and compression of double-notched specimen test methods.

In 1999 a round-robin testing program was completed in the U.S. to determine the precision of ASTM test standard C1292 [80]. From this study coefficients of variation for repeatability and reproducibility were obtained for in-plane and interlaminar shear strength of CG-Nicalon/PIP SiNCO. Figures 22.19 and 22.20 summarize the results obtained by the various laboratories that participated in this testing program. These plots also

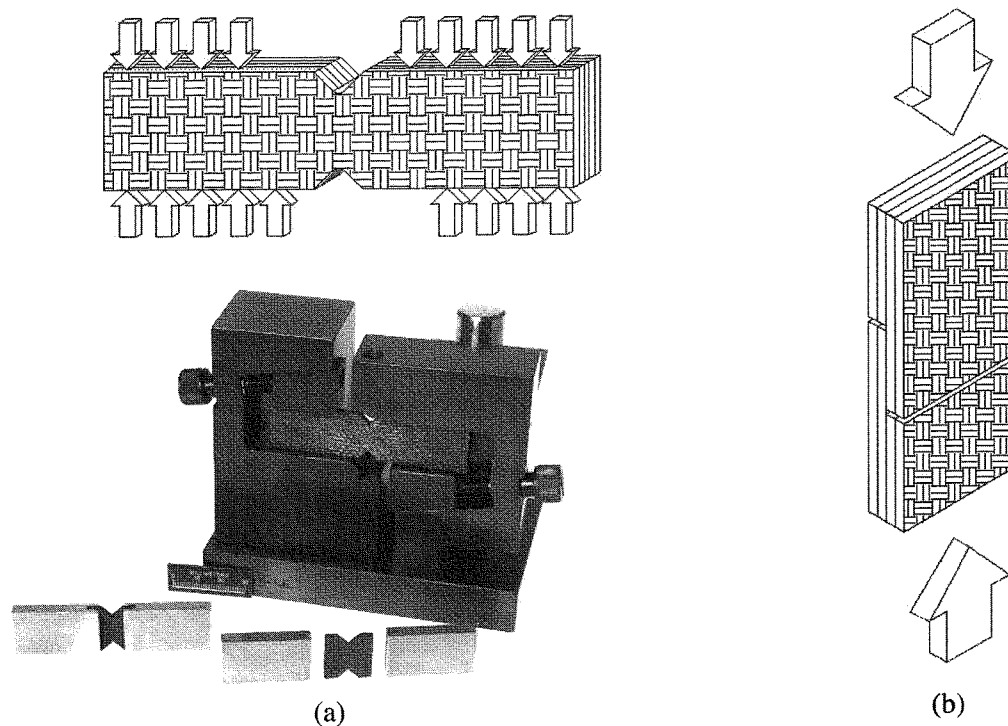


Figure 22.18 (a) Schematic and Fixture for Iosipescu Test for Determination of In-Plane and Interlaminar Shear Strength. (b) Schematic of Compression of Double-Notched Specimen for Determination of Interlaminar Shear Strength.

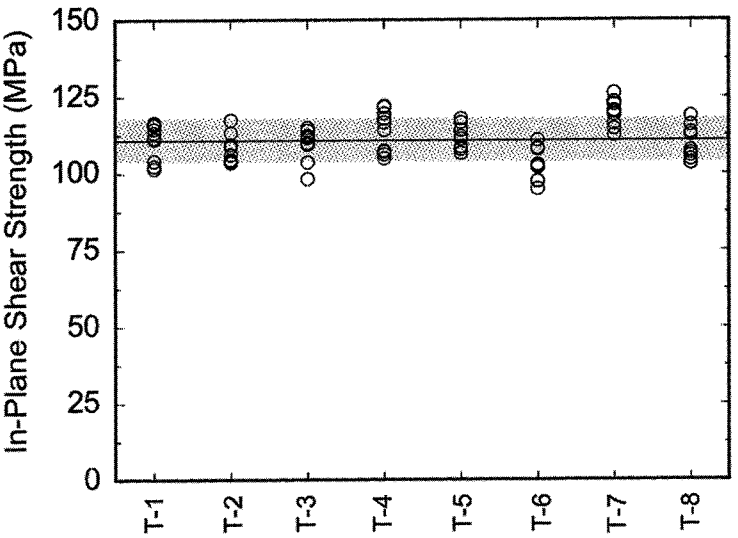


Figure 22.19 Summary of In-Plane Shear Strength Results for CG-Nicalon™/BN/SiNCO CFCC Obtained from Round-Robin Testing Program by Iosipescu Test Method. Notch Separation Was 11 mm [80].

show the value of the great mean and one standard deviation with respect to that value. Although the in-plane shear strength results show little variability, the interlaminar shear strength results exhibited significant variability. This large degree of variability is associated with the variation in the microstructure of the material and with the relative location of the roots of the notches with respect to the interlaminar region of the material. Figure 22.21 shows photographs of a double-notched specimen, used for the determination of interlaminar shear

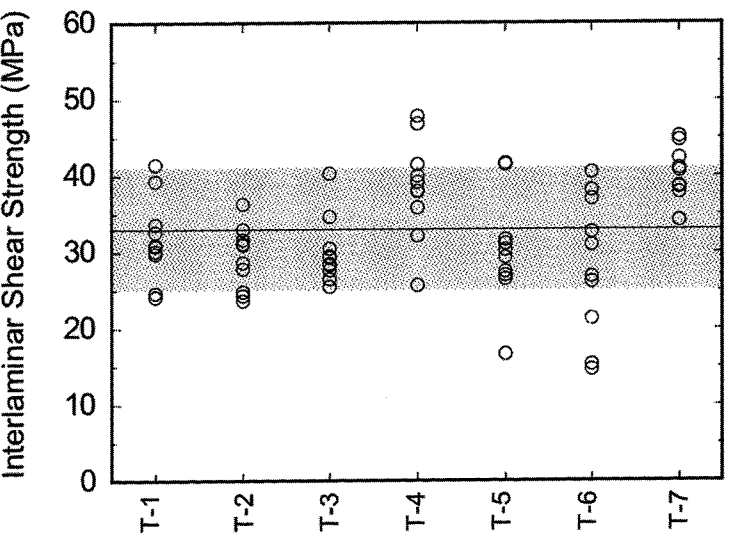


Figure 22.20 Summary of Apparent Interlaminar Shear Strength Results for CG-Nicalon™/BN/SiNCO CFCC Obtained from Round-Robin Testing Program by Compression of Double-Notched Specimens. Notch Separation Was 6 mm [80].

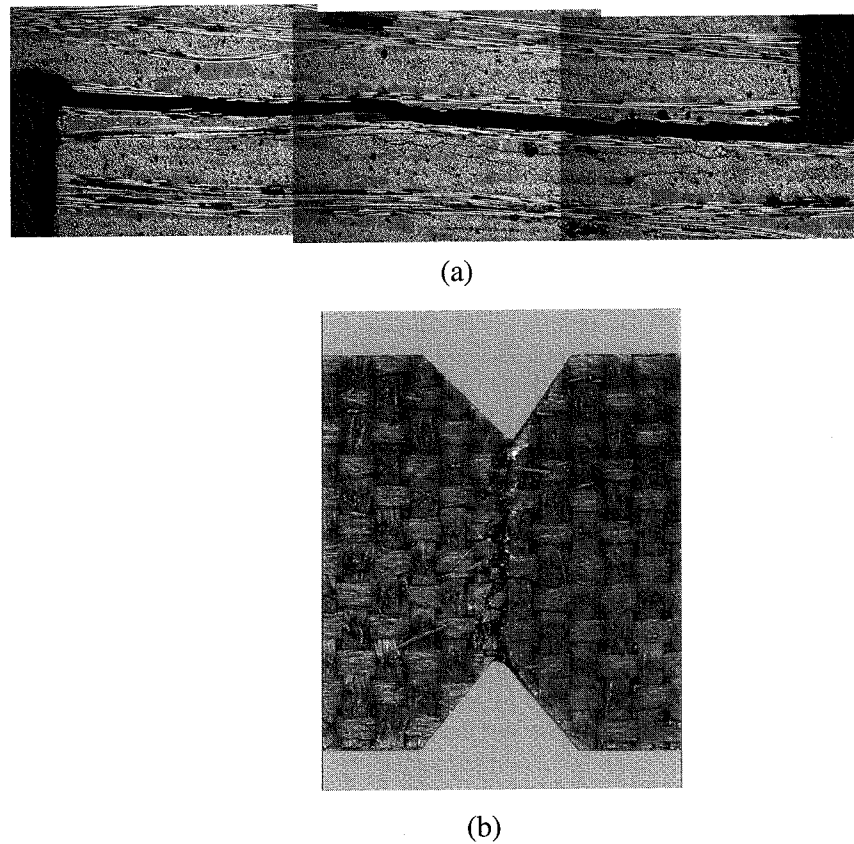


Figure 22.21 (a) Micrograph of CG-Nicalon™/BN/SiNCO CFCC Double-Notched Specimen After Test Illustrating the Propagation of Interlaminar Crack between Notches.
 (b) Micrograph of CG-Nicalon™/BN/SiNCO CFCC Iosipescu Specimen After Test [96].

strength, and of an Iosipescu specimen used for the determination of in-plane shear strength, after testing. Figures 22.22 and 22.23 contain interlaminar shear strength results for various CFCCs at ambient temperature as a function of notch separation and elevated temperature, respectively, while Tables 22.2 and 22.3 list additional results. In the case of Hi-Nicalon™/BN/MI-SiC CFCCs, the decrease of interlaminar shear strength with temperature shown in Figure 22.23 is associated with degradation of the fiber/matrix interfacial region [99].

Fracture Resistance

The main reason why CFCCs are preferred over monolithic ceramics for use in structural applications is the ability of the former to redistribute stresses around notches [101]. Failure mechanisms and processes in CFCCs during stable fracture are not merely confined to a localized region at the crack tip but include crack bridging, crack deflection, multiple matrix cracking and fiber pull-out over a larger fracture process zone [102, 103]. As a consequence, the nature of the fracture process in these materials precludes the application of linear elastic fracture mechanics (LEFM). In spite of this, many authors have made, and continue making use of existing LEFM formalisms for the analysis of fracture resistance of CFCCs. Others have made use of concepts such as equivalent elastic crack and R-curves, which characterize a material's resistance to fracture during slow, stable crack propagation and are dependent on the nature of the process zone extending from the crack tip in the material. Table 22.4 lists fracture resistance parameters obtained from the evaluation of various CFCCs.

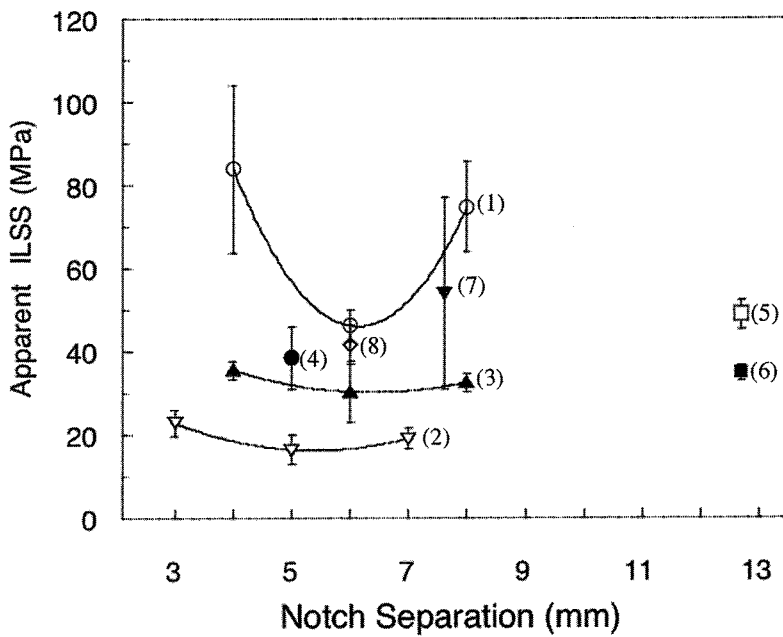


Figure 22.22 Effect of Notch Separation on the Interlaminar Shear Strength of 2-D CVI-SiC Matrix Composites: (1) CG-Nicalon™, 0.3 µm Carbon Fiber Coating [97]. (2) CG-Nicalon™, 1.1 µm Carbon Fiber Coating [97]. (3) CG-Nicalon™, Boron Nitride Fiber Coating, SiNCO Matrix [96]. (4) CG-Nicalon™ [75]. (5) CG-Nicalon™, 0.1 µm Carbonaceous Fiber Coating [88]. (6) T300 Carbon Fiber 0.1 µm Carbonaceous fiber coating [88]. (7) CG-Nicalon™, 0.1 µm Carbonaceous Fiber Coating [98]. (8) Hi-Nicalon™, Dual Boron Nitride-CVD-SiC Fiber Coating, MI-SiC Matrix [99].

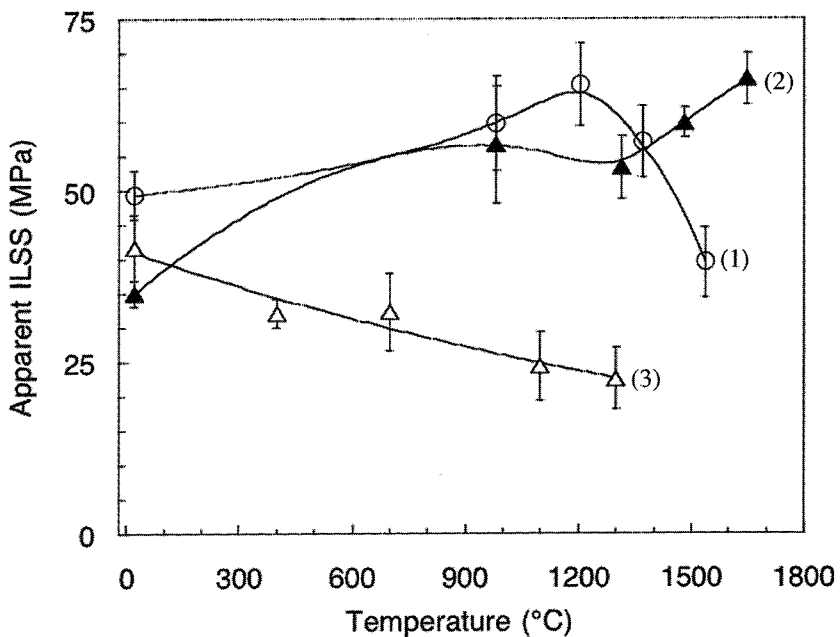


Figure 22.23 Effect of Temperature on the Interlaminar Shear Strength of: (1) CG-Nicalon™/C/CVI-SiC in Helium. (2) T300 carbon/C/CVI-SiC in Helium [88]. (3) Hi-Nicalon™/BN/MI-SiC in Air [99].

TABLE 22.2 IN-PLANE SHEAR STRENGTH OF CFCCCs

Fiber	Matrix	Interface	V _f (%)	Fiber Architecture	Method	Porosity (%)	Density (g/cm ³)	Shear Strength (MPa)	Proportional Shear (MPa)	Failure Shear Strain (%)	Reference
CG-Nicalon™	CVI-SiC	0.3 µm PyC	40	PW (0/90)	Iosipescu	15-20		101 (4.7)*			[100]
CG-Nicalon™	PIP SiNCO	0.5 µm BN	42-48	8HSW (0/90)	Iosipescu			110.8 (6.8)			[80]
CG-Nicalon™	CVI-SiC	PyC	33	8 plies 8HSW (0/90)	Iosipescu		2.54	95.8 (11.0)	39.3 (6.2)	0.62 (0.05)	[75]
				8 plies 8HSW (0/90/±45)			2.54	114.5 (11.7)	40.7 (9.)	0.55 (0.03)	
				8 plies 8HSW (±45)			2.54	124.1 (8.3)	44.1 (9.0)	0.50 (0.02)	
Nextel™ 720	AS		48				2.6	30.9	0.49		[81]

* Specimens 76 mm long, 19 mm wide and the separation between notches was 11 mm.

TABLE 22.3 INTERLAMINAR-PLANE SHEAR STRENGTH OF CFCCCs

Fiber	Matrix	Interface	V _f (%)	Fiber Architecture	Method	Porosity (%)	Density (g/cm ³)	Shear Strength (MPa)	Reference
CG-Nicalon™	CVI-SiC	0.3 µm PyC	40	12 layers PW (0/90)	DNS	15-20			[91]
Nicalon™	PIP Si-N-C-O	0.5 µm BN	42-48	8HSW (0/90)	DNS			33.0 (8.0)**	[80]
CG-Nicalon™	CVI-SiC	PyC	33	8 plies 8HSW (0/90)	DNS		2.54	38.6 (7.6)*	[75]
				8 plies 8HSW (0/90/±45)				40.7 (5.5)	[75]
				8 plies 8HSW (±45)				41.4 (9.0)	
Nextel™ 720	AS		48				2.6	11.5	[81]
T300	CVI-SiC	PyC	45				2.1	19-35***	[98]
CG-Nicalon™	MI-SiC	BN	40	8HSW 0/90	DNS		2.5	32-77***	[99]

* compression of double-notched specimens (50 mm × 20 mm) with a notch separation of 5 mm using an anti-buckling fixture.

** Round robin testing program. 80 tests by 8 laboratories using double notched specimens

***The dimensions of the specimens were: 20.3 mm in length and 10.15 mm in width, while the notch separation was 7.62 mm.

TABLE 22.4 FRACTURE BEHAVIOR OF CFCCs

Fiber	Matrix	Interphase	V _f (%)	Fiber Architecture	Method	Porosity (%)	Density (g/cm ³)	Fracture Parameter	Reference
CG-Nicalon™	CVI-SiC	PyC	PW 0/90	Chevron-notched bend specimens			2.6–2.8 kJ/m ³		[103]
CG-Nicalon™	CVI-SiC	PyC	32	3-D braided	SENB 3-pt SENB ASTM E399	11	2.6	30–35 MPa.m ^{0.5}	[104]
CG-Nicalon™	CVI-SiC	PyC					29.8 (2.5) MPa.m ^{0.5}		[105]
CG-Nicalon™	CVI-SiC	PyC					18.1 (0.7) [‡] MPa.m ^{0.5}		
CG-Nicalon™	CVI-SiC	PyC					13.3 (1.0) MPa.m ^{0.5}		
T300	CVI-SiC	PyC	35	PW 0/30/60		15	2.3	10.0 (1.2) [‡] MPa.m ^{0.5}	
T300	CVI-SiC	PyC					16.2 (1.7) [†] MPa.m ^{0.5}		
CG-Nicalon™	CVI-SiC	PyC					11.9 (0.7) [‡] MPa.m ^{0.5}		
T300	CVI-SiC	PyC					8.2 (0.5) [†] MPa.m ^{0.5}		
T300	CVI-SiC	PyC	40	3D	SENT 3-pt SENB ASTM E-813	15–20	6.8 (1.0) [‡] MPa.m ^{0.5}		[106]
CG-Nicalon™ **	CVI-SiC	ML C/SiC			CT J-Integral		22.1 (33.5) MPa.m ^{0.5}		[107]
CG-Nicalon™ **	CVI-SiC	ML C/SiC			CT		11.4–16.5*		[108]
CG-Nicalon™	CVI-SiC	PyC	33	8 plies 8HSW (0/0/90)			30.9		[109]
CG-Nicalon™	CVI-SiC	PyC		8 plies 8HSW (0/90/±45)			12–30 kJ/m ²		[109]
CG-Nicalon™	CVI-SiC	PyC	40	PW 0/90			10		[109]
CG-Nicalon™	CVI-SiC	PyC		PW 0/90			27.7 (1.0) MPa.m ^{0.5}		[109]
CG-Nicalon™	CVI-SiC	PyC					2.54		[109]
CG-Nicalon™	CVI-SiC	PyC					29.9 (1.1) MPa.m ^{0.5}		[109]
CG-Nicalon™	CVI-SiC	PyC					27.6 (0.6) MPa.m ^{0.5}		[109]
CG-Nicalon™	CVI-SiC	PyC					14		[110]
CG-Nicalon™	CVI-SiC	PyC					14		[111]
CG-Nicalon™	CVI-SiC	PyC					14–27***		[112]
							12–18		

1. In 1-3 plane

2. In 1-2 plane

† After heat treatment at 1200°C for 100 hours in air.

* Specimens 76 mm long, 19 mm wide and the separation between notches was 11 mm.

** Proprietary fiber surface treatment

*** 1200°C in air.

The resistance of CFCCs to crack propagation can also be evaluated by the notch sensitivity test. In this case, test specimens with notches or holes of different depth or diameter, are evaluated in tension and the results are compared with those of test specimens without notches or holes. The tensile strength values as a function of notch depth or hole diameter allow the determination of the range of notch sizes for which the material is sensitive to the presence of notches. Figure 22.24 contains a photograph of a NextelTM720/AS specimen with a hole, which was used as part of a study to assess the notch sensitivity of this material. Figure 22.25 contains a plot of normalized strength as a function of the ratio of hole diameter (or notch length) to specimen width for CG-NicalonTM/CVI-SiC and NextelTM610/AS. The line associated with notch insensitivity is also included in that plot. These results suggest that both of these CFCCs exhibit mild notch sensitivity and that in the case of the all-oxide CFCCs, it becomes more notch-sensitive at high-temperature. Figure 22.26 contains a plot of tensile strength results versus the ratio of hole diameter to width, for NextelTM720/AS CFCCs. These results suggest that this CFCC is effectively notch insensitive in the as-processed condition and that its strength exhibits a mild dependence on volume (specimen width). However, after an ageing treatment at 1100°C for 100 hrs the strength of this material decreases and the material becomes notch sensitive. Figure 22.27 presents results of the net section strength versus hole diameter for a NextelTM610/mullite-alumina CFCC, which suggest that this CFCC exhibits mild notch sensitivity and modest dependence of strength with hole size [79].

The evaluation of notched test specimens is also of interest because some gas turbine engine components (e.g.—combustor liners, flaps and seals) contain cooling holes and bolted attachment points [115].

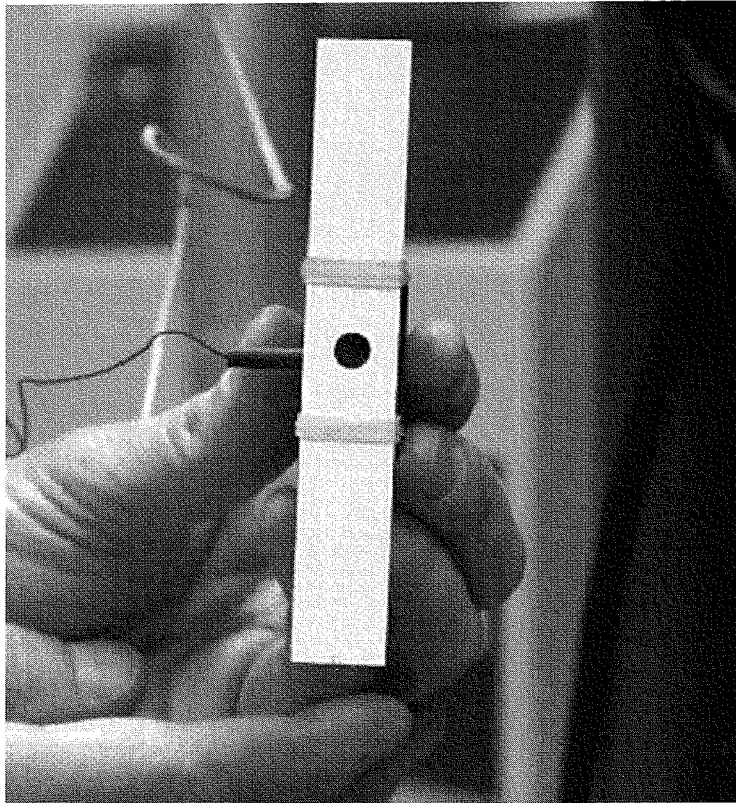


Figure 22.24 Photograph of All-Oxide Tensile Specimen with Hole Utilized for Determination of Notch Sensitivity of CFCCs

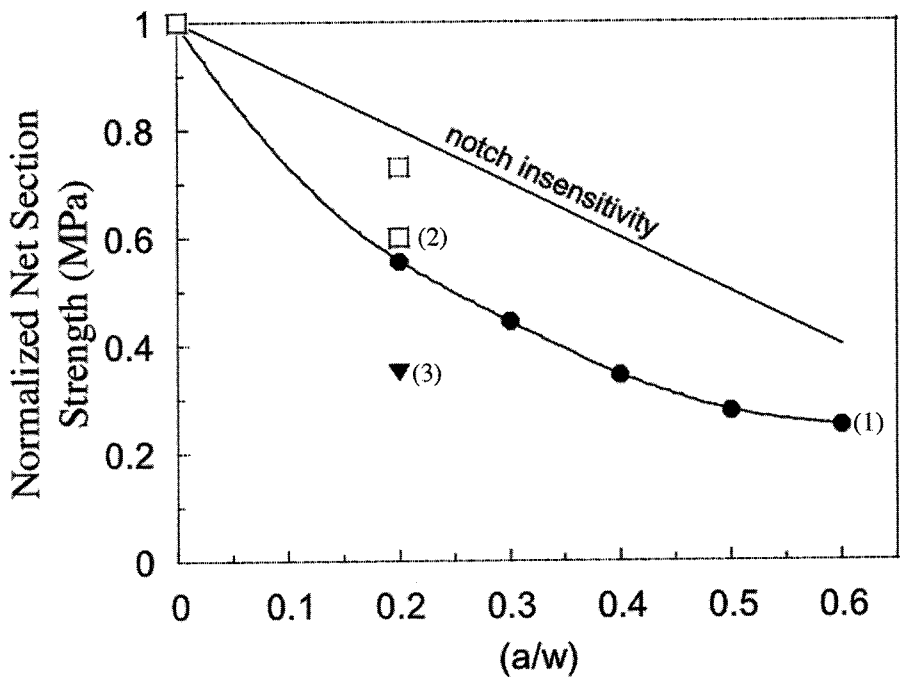


Figure 22.25 Notch Sensitivity of: (1) CG-Nicalon™/C/CVI-SiC [106], (2) Nextel™610/AS (23°C), and (3) Nextel™610/AS (950°C) [113].

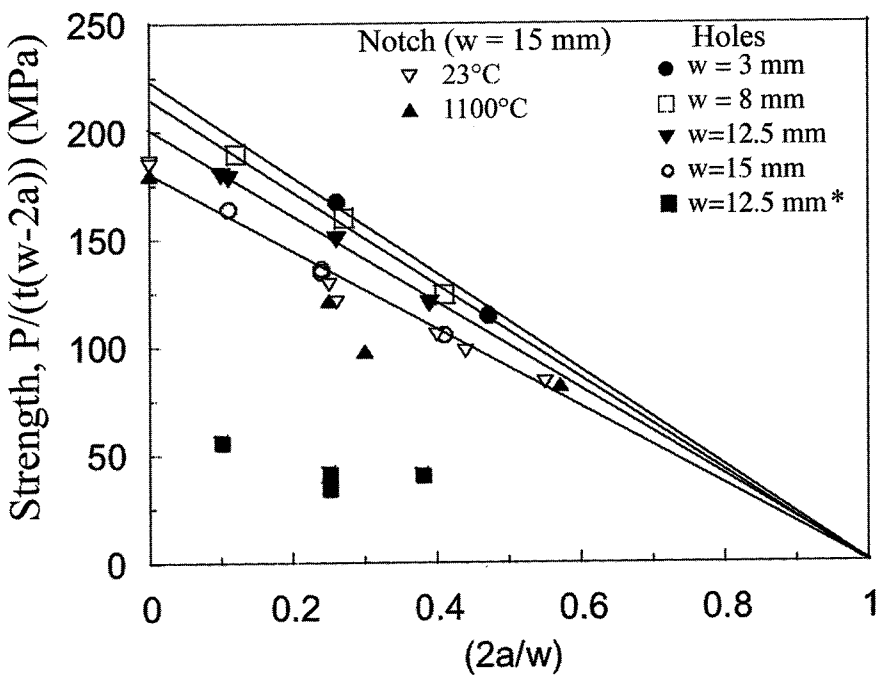


Figure 22.26 Notch Sensitivity Behavior of Nextel™720/AS: Specimens with Holes of Diameter $2a$: * Indicates that Specimen was Tested after Aging at 1100°C for 100 hrs [114]. Double-Notched Specimens of $w = 15$ mm and Notches of Length a [115]. The Solid Lines Correspond to Notch Insensitive Behavior for Each Specimen Width.

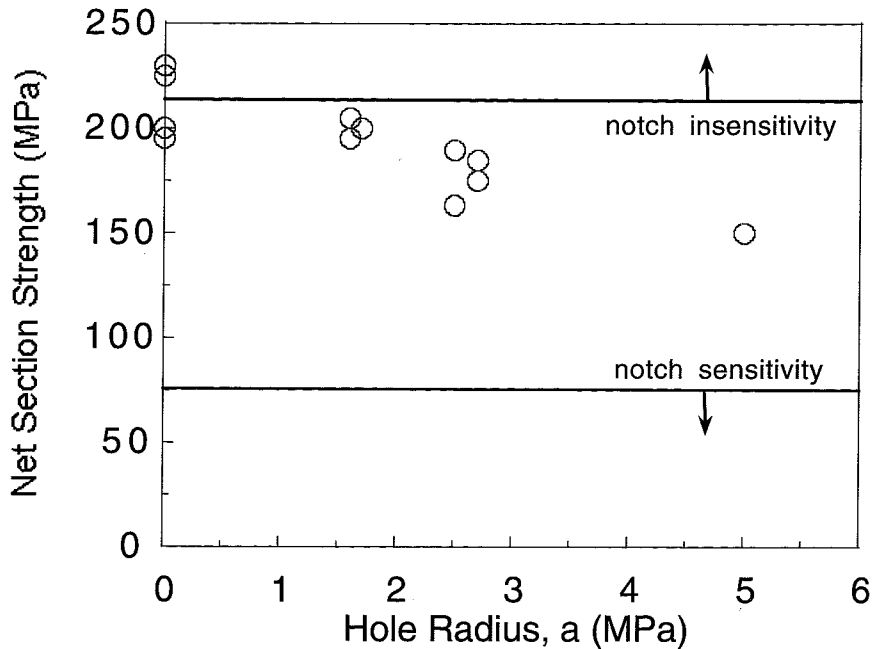


Figure 22.27 Effect of Hole Size on the Notch-Sensitivity of Center-Hole Tensile Specimens of Nextel™610/Mullite-Alumina CFCC [79]

PHYSICAL PROPERTIES

Transport Properties

When used in gas turbine engines CFCCs will be subjected to high temperatures, high heat fluxes and thermal gradients. Thermal gradients will induce thermal strains and consequently stresses. Among the various material properties that affect the magnitude of these thermal strains and stresses, thermal conductivity is the most important one [116]. In general, high values of thermal conductivity are desirable to minimize thermal stresses and strains, but the opposite would be true for applications requiring energy conservation. Although the thermal conductivity of CFCCs is independent of the environment, it becomes dependent when fiber-matrix debonding occurs and the environment can ingress in the interfacial region. It has also been found that the thermal diffusivity parallel to the fiber direction of composites exceeds the corresponding values for heat flow perpendicular to the fibers [116].

Figure 22.28 presents data for the temperature-dependence of thermal conductivity of CG-Nicalon™/CVI-SiC and values for Sylramic/MI-SiC composite with or without CVI-BN interface. Table 22.5 lists results for other CFCCs.

Thermal Expansion

Thermal expansion is one of the most important properties for the selection of materials for high-temperature applications. Volumetric changes with temperature become a prime consideration when materials with dissimilar thermal expansion values are incorporated in designs because thermally-induced stresses are proportional to the difference in the coefficients of thermal expansion. Table 22.6 lists values of thermal expansion for various CFCCs.

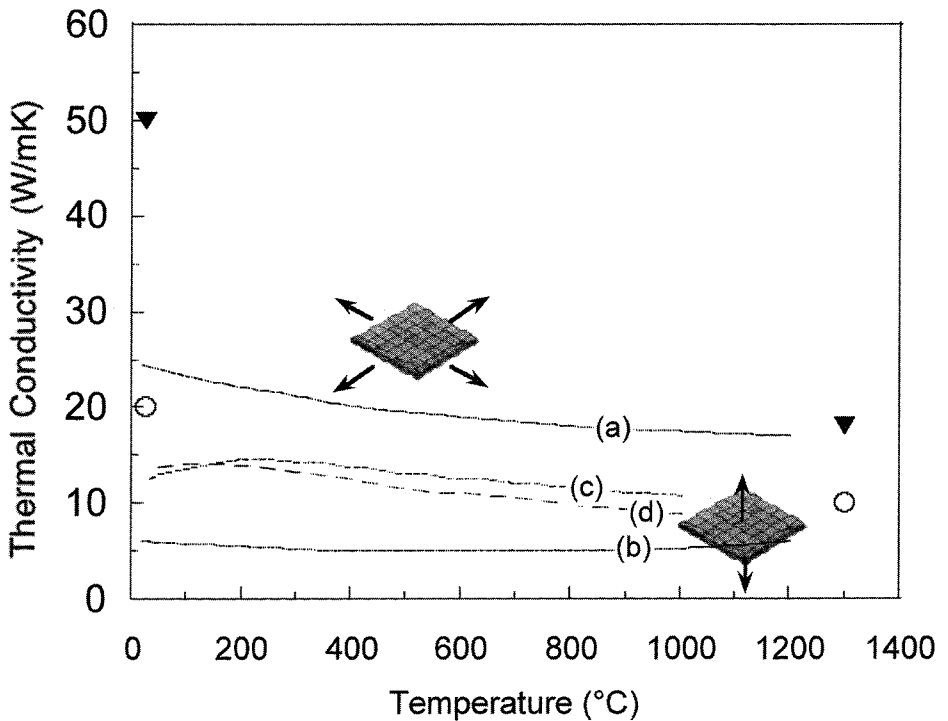


Figure 22.28 Thermal Conductivity of 2-D CG-Nicalon™ Fiber-Reinforced CVI-SiC Matrix Composites. (a) Parallel to Fiber Direction (b) Perpendicular to Fiber Direction [86]. (c) Parallel to Fiber Direction with a Carbonaceous Fiber Coating, 1 μm Thick; (d) Parallel to Fiber Direction with a Carbonaceous Fiber Coating, 0.1 μm thick [117]; Open Circle: Through-the-Thickness Thermal Conductivity of Sylramic/MI-SiC Composite with CVI-BN Interface; Closed Triangle: Through-the-Thickness Thermal Conductivity of Sylramic/MI-SiC Composite Without CVI-BN Interface [118].

Thermal Shock Resistance

Shutdowns for either scheduled or unscheduled maintenance will result in a decrease in the temperature of, and stress build-up in, hot-section components of gas turbine engines. The magnitude of these stresses will depend on the cooling rate and on the magnitude of thermal gradients. To be used in the hot section of gas turbine engines, CFCCs must possess adequate resistance to thermal shock in order to survive transients (e.g.—flame outs, which would subject hot components to thermal shock by incoming cold compressed air in the combustor) [124]. Traditionally, thermal shock conditions can be simulated in the laboratory using either water or air quenching after exposure to a furnace environment. However, more extreme thermal shock conditions have been obtained using stationary rocket engines [125].

In general CFCCs exhibit good thermal shock resistance. Damage resulting from thermal shock in CG-Nicalon™/SiC has been associated with microcracks that initiate from pores in the matrix, growth of cracks inside and between bundles in the transverse plane, and saturation of microcracks after repeated quenching [126, 127]. C/SiNCO and SiN-SiNCO CFCCs, which were used to fabricate scrolls in a 100 kW automotive gas turbine engine, have demonstrated excellent thermal shock resistance after being subjected repeatedly to high-temperature (1350°C) and high-speed (100 m/s) gas flow, followed by cold gas flow (20 m/s) [32].

TABLE 22.5 TRANSPORT PROPERTIES

Fiber	Matrix	Interface	V _f (%)	Fiber Architecture	Method	Porosity (%)	Density (g/cm ³)	Thermal Diffusivity (10 ⁻⁶ m ² /s)	Thermal Conductivity (Wm ⁻¹ K ⁻¹)	Reference
CG-Nicalon™	CVI-SiC	0.03–1.0 µm PyC	39.5–43.7	PW (0/30/60)	Xenon flash lamp	15–20	2.22–2.65	8.4–12.9*	7.4 ≈	[119]
Hi-Nicalon™	CVI-SiC	0.3 µm PyC	40	PW (0/30/60)	Xenon flash lamp	15–20	2.22–2.65		25.3 ≈	[120]
CG-Nicalon™				PW (0/30/60)					6.8 ≈	
Amoco K100, P55	—	—	44**	3D				24.7 ≈		
CG-Nicalon™	CVI-SiC	PyC		PW (0/30/60)				12 ≈		
								5.6 ± 0.6		[121]

*The transverse thermal conductivity (which was calculated using the estimated composite specific heat obtained from the application of the rule of mixtures) increased with increasing carbon coating thickness from 8.4 Wm⁻¹ K⁻¹ for 0.03 µm to 12.9 Wm⁻¹ K⁻¹ for thickness of 1 µm while the thermal conductivity for a material without fiber coating was found to be 13.4 Wm⁻¹ K⁻¹.

** P55 fibers were woven in the x and y directions with 2000 fibers/tow, while six tows (1000 fibers/tow) of K1100 fibers were woven through the orthogonal weave in the perpendicular direction (z). The overall fiber volume fraction was 44% of which 7% was in the x and y directions and 86% was in the z-direction.

*** Thermal diffusivity values were obtained after specimens were subjected to thermal shock (in water) for ΔT = 0, 200, 400, 600, 800 and 1000°C. Another specimen was water-quenched 4 times at DT = 800°C. The thermal diffusivity was found to remain constant (within scatter) regardless of quench history.

TABLE 22.6 THERMAL EXPANSION

Fiber	Matrix	Interphase	V _f (%)	Fiber Architecture	Method	Porosity	Density g/cm ³	Coefficient of Thermal Expansion 10 ⁻⁶ K ⁻¹	Reference
CG-Nicalon™	CVI-SiC		0.26	4HSW	Dual Dilatometer	2.47	5.30 ± 0.03		[122]
Nexel™ 312			0.34	8HSW		1.98	4.77 ± 0.04		
FP® alumina			0.31	8HSW		1.90	4.45 ± 0.07		
Nextel™ 720	AS	—	40	8HSW	Extensometer		5.3 (200°C–700°C)		[10]
T300	MI-SiC	C	38	8HSW	Extensometer		6.6 (700°C–1000°C)		[123]
							2.5 (200°C–600°C)		
							2.8 (400°C–800°C)		
							3.2 (600°C–1000°C)		

DURABILITY AND RELIABILITY

Matrix Cracking

Matrix cracking of CFCCs is very dependent on the microstructure of the composite, fiber properties, fiber architecture, porosity and residual stresses. Because matrix cracks in non-oxide matrix CFCCs can serve as avenue for the ingress of the environment into the interior of the composite, which may result in degradation and loss of strength, the matrix cracking stress is considered as the maximum allowable design stress for these CFCCs.

The various stages of matrix cracking in 2-D CVI-SiC CFCCs during tensile testing have been well identified [128, 129]. Microcracks tend to initiate first at singularities around macropores at 0.025% deformation, and then propagate across neighboring longitudinal yarns to the nearest macropores. Saturation of macropore-originated microcracks occurred at 0.12% deformation. At larger deformation levels, microcracks form in the transverse yarns and in the narrow strips of interply matrix located between macropores. The formation of these microcracks stops at 0.2% deformation, but microcracks appear randomly in the matrix surrounding the longitudinal bundles for deformations above 0.2% [130].

For many gas turbine engine components, resistance to foreign object impact damage is of critical concern, because catastrophic failure of components can lead to catastrophic engine failure. Limited studies have been focused on studying the resistance of CFCCs to foreign object impact. However, existing results indicate that the tensile strength of CG-Nicalon/CVI-SiC remains unchanged after impact with 1.0 mm diameter zirconia spherical particles at speeds of 600 m/s [32, 131]. Only a spalling crater and radial cracks were caused by the impact and the impact site was not the origin of the composite failure. However, at elevated temperatures in aggressive environments, formation of cracks resulting from foreign object impact could serve as avenues for the ingress of the environment into the material, which in turn would lead to degradation of properties and failure.

Mechanical Cyclic Fatigue

During service in gas turbine engine CFCCs will be subjected to variable thermal and mechanical loading. However, the microstructural features and damage mechanisms that are responsible for the tough behavior of CFCCs (i.e., low interfacial shear stress, long fiber debond lengths and matrix microcracking) often conflict with the microstructural requirements for optimal fatigue resistance [132].

In general, fatigue-induced failure of continuous fiber-reinforced ceramics is governed by interface wear, fiber damage and matrix crack growth [133]. Moreover, these damage processes are enhanced at elevated temperatures, particularly when the fibers and fiber coating are susceptible to corrosion/oxidation. It has been found that at ambient temperature the fatigue limit of CFCCs decreases with increasing frequency [134] and that the residual monotonic tensile strength of some CFCCs increases after reaching fatigue endurance. This phenomenon has been explained as the result of decreasing stress concentrations near the cross-over points between the 0° and 90° bundles.

Figure 22.29 contains a plot of peak stress versus number-of-cycles plot containing results for various CFCCs at various temperatures. In most cases, the life of CFCCs decreases with increasing peak fatigue stress. At peak fatigue stresses below the proportional stress limit, CFCCs exhibit endurance [138]. Limited work has been carried out to evaluate the thermomechanical fatigue of CFCCs [139, 140], but information obtained from this type of tests will be necessary to develop a thorough understanding of the behavior of CFCCs during transient operation of gas turbine engines.

Creep, Stress-Rupture and Stress Relaxation

When materials and structures are subjected to constant tensile loads at high homologous temperatures, they will experience dimensional changes with time. Although the resulting elongation of CFCCs is often referred to as "creep" deformation, it arises not only from the viscous deformation of the composite

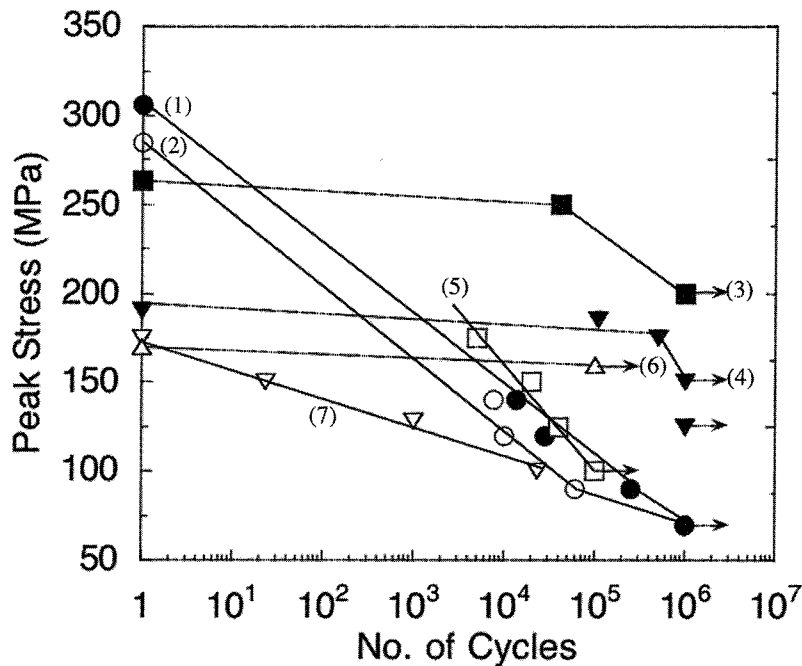


Figure 22.29 Fatigue Behavior of CFCCs in Air. (1) CG-Nicalon™/BN/(PIP-SiNCO + 25% SiC), 982°C [135]. (2) CG-Nicalon™/BN/(PIP-SiNCO + 25% SiC), 1204°C [135]. (3) CG-Nicalon™/BN/(PIP-SiNCO + 25% SiC), 23°C [135]. (4) CG-Nicalon™/BN/PIP-SiNCO, 23°C [136]. (5) CG-Nicalon™/BN/PIP-SiNCO, 1000°C [136]. (6) Nextel™720/AS, 1000°C [137]. (7) Nextel™720/AS, 1200°C [137].

constituents (e.g.—creep deformation), but also from matrix cracking, fiber debonding, fiber sliding and fiber failure. At elevated temperatures, time-dependent matrix cracking [141,142] (with the consequent compliance changes) can occur at composite stresses lower than the monotonic proportional limit stress at that particular test temperature as a result of dissimilar creep resistance of the constituents [92,143–145].

Figure 22.30 contains a series of tensile creep curves for CG-Nicalon™/PIP-SiNCO at 1200°C. In general, the amount of deformation and the rate of deformation of CFCCs increases with temperature and applied tensile stress. The curves in Figure 22.30 exhibit continuously decreasing rate of deformation with increasing time/deformation and in most cases the rate of deformation never reaches a true minimum value. Exceptions occur when due to cumulative fiber failure the effective load bearing capability of the CFCC in the plane of the critical crack is reduced. In this case CFCCs exhibit accelerated deformation analogous to “tertiary creep” in metals [146–148].

The magnitude of the rate of deformation of CFCCs is influenced by the rate of deformation of the constituents, the rate of load redistribution among them, which results from their differential creep resistance, and changes in compliance due to matrix cracking and fiber failure. Figure 22.31 illustrates the effect of fiber type on the creep deformation of PIP-SiNCO matrix composites. It can be observed that PIP-SiNCO matrix composites reinforced with Hi-Nicalon™ fibers are two orders of magnitude more resistant to creep deformation than PIP-SiNCO matrix composites reinforced with CG-Nicalon™ fibers. Hi-Nicalon™ fibers are processed through e-beam curing and therefore contain a lower amount of oxygen (below 0.5% wt) than CG-Nicalon™ fibers. As a result of this modification in processing, Hi-Nicalon™ fibers are stiffer, much more creep resistant than CG-Nicalon™ fibers and experience little of the strength degradation experienced by CG-Nicalon™ fibers at high-temperatures due to the decomposition of the oxycarbide phase.

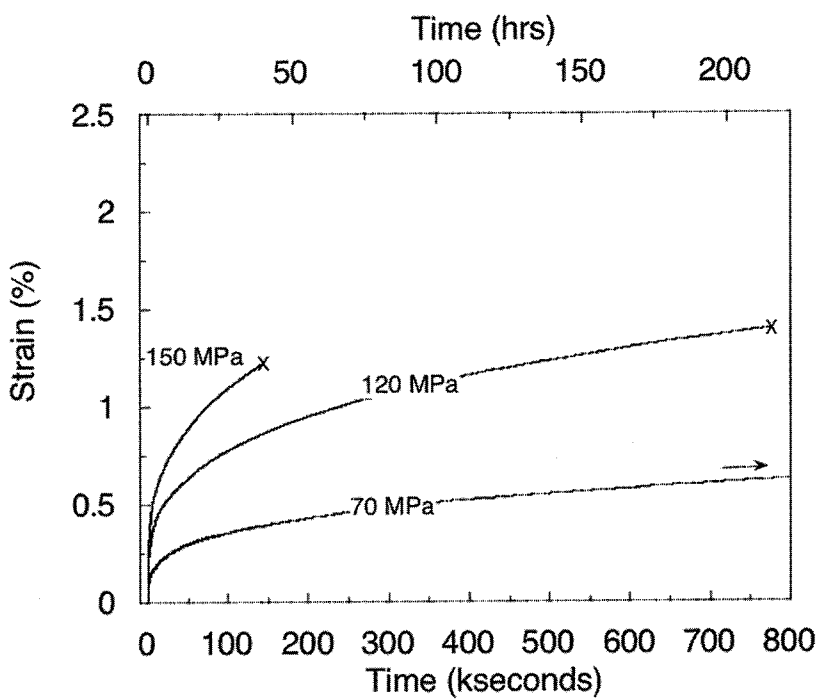


Figure 22.30 Tensile Creep Strain in Air at 1200°C for CG-Nicalon™/BN/SiNCO

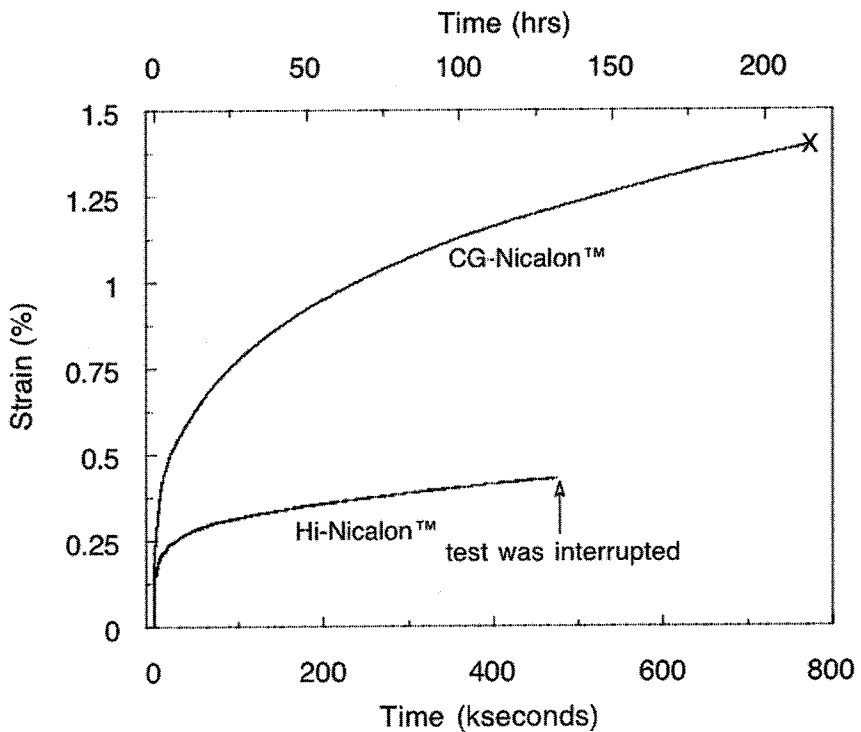


Figure 22.31 Effect of Fiber Type (CG-Nicalon™ versus Hi-Nicalon™) on the Creep Resistance of SiNCO Matrix CFCCs in Air at 1200°C. It is Effectively One Order of Magnitude Increase in Creep Resistance [97].

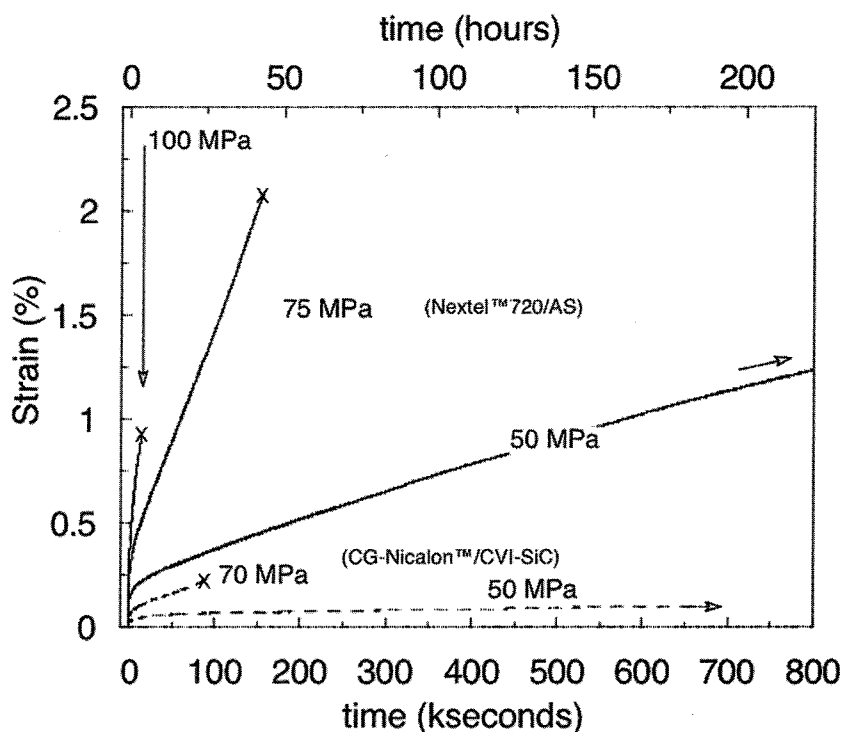


Figure 22.32 Tensile Creep Strain in Air at 1200°C for CG-Nicalon™/C/CVI-SiC and Nextel™720/AS [150]. Test at 50 MPa for CG-Nicalon™/C/CVI-SiC was Interrupted.

In general, SiC-based fibers are stronger than oxide fibers at room temperature and retain more of their strength at elevated temperatures. Oxide fibers are stiffer than many SiC-based fibers at room temperature, but they lose their stiffness advantage above 1000°C [149]. Although oxide fibers are more stable than SiC-based fibers in oxidizing environments at high temperatures, they experience grain growth and loss of strength due to softening of their grain boundaries[7–10, 149].

Figure 22.32 contains a plot with creep curves for CG-Nicalon™/CVI-SiC and Nextel™ 720/AS CFCCs at 1200°C in air. These results demonstrate that under the same conditions, the former is at least one order of magnitude more resistant than the latter. However, at stresses above the matrix cracking stress of CG-Nicalon™/CVI-SiC, its life is significantly shorter than that of Nextel™ 720/AS. This is the result of degradation in the interior of CG-Nicalon™/CVI-SiC from oxidation of the fiber coating and fibers, which leads to fiber failure and rupture of the CFCC.

An analysis of stress-rupture results for CG-Nicalon™/CVI-SiC CFCCs at temperatures between 600°C and 1000°C has shown that strength of this material decreases with time according to [151,152]

$$\sigma = C_3 t_f^{-0.25} \quad (2)$$

where σ denotes the tensile strength, C_3 is a constant and t_f is the time-to-failure. This time-dependence of CFCC strength is consistent with models based on the oxidation of the reinforcing fibers and the nucleation of notches or flaws in the oxide layer [146,148,150]. Similar models have been formulated to explain the stress-rupture of all-oxide CFCCs as a result of grain growth in the fibers and loss of fiber strength [10]. These models have also been able to predict the time-dependent changes in material compliance during

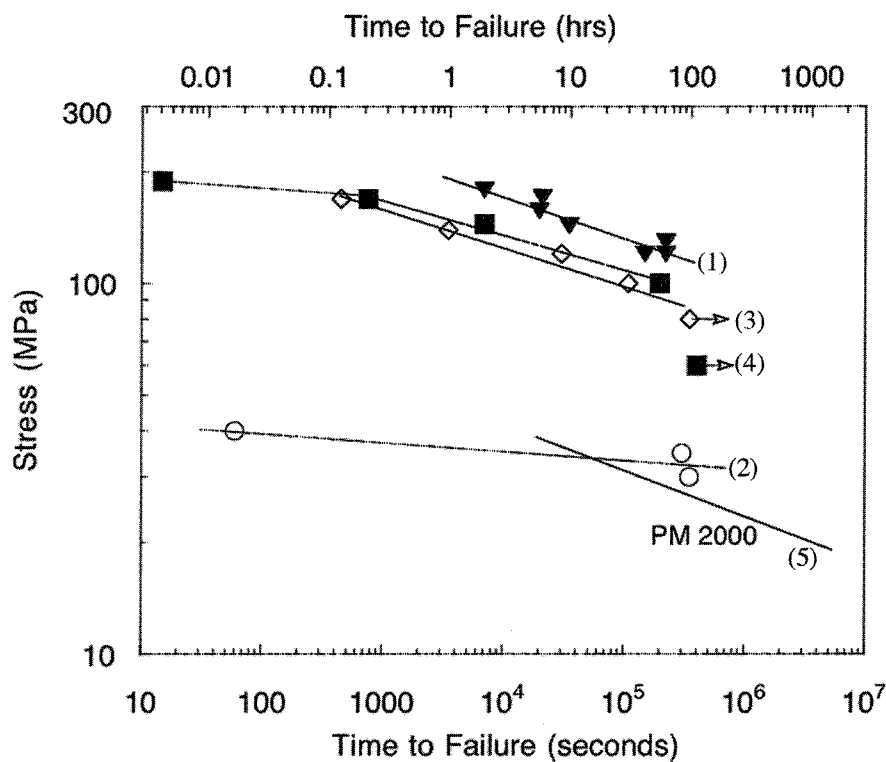


Figure 22.33 Plot of Stress (MPa) versus Time-to-Rupture for Tests Conducted in Air at 1300°C for: (1) 3-D Tyranno Lox-M/C/Si-Ti-C-O [153]. (2) 2-D, CG-Nicalon™/CVI-SiC [154]. (3) 2-D, Hi-Nicalon™/CVI-SiC [154]. (4) 2-D, CG-Nicalon™/“Enhanced” SiC [154]. (5) Data for PM2000.

stress-rupture conditions, which in addition to creep (e.g.—viscous deformation) result from the progressive oxidation of the fiber coating, the redistribution of stresses in the fibers bridging matrix cracks, the oxidation of the fibers and ultimately fiber failure [150].

In general, the stress-rupture behavior of CFCCs currently available is better than that of many metallic materials (other than single crystals) currently used in gas turbine engine applications. Figures 22.33–22.35 present stress-rupture data for several CFCCs in air at temperatures between 1100°C and 1300°C. In general, at these temperatures the strength of CFCCs decreases with time and temperature¹. For comparative purposes, data are also included for several metallic alloys.

In many gas turbine engine applications, stresses are thermally-induced. To assess the potential of candidate CFCCs for these applications it is more appropriate to carry-out tests under strain-controlled conditions, rather than under load-controlled conditions (e.g.—creep, stress-rupture). Figure 22.36 illustrates the stress-relaxation behavior of Sylramic®/PIP-SiNCO when subjected to increasingly larger strains values at 1300°C in air. These results show that the material is able to relax as much as 80% of the stress associated with the

¹At intermediate temperatures (e.g.—between 600°C and 950°C) many SiC-based CFCCs exhibit “anomalous” behavior, i.e.—they are less resistant to stress-rupture in air at those temperatures than at 1100°C. When plotting failure time versus temperature at constant stress, the resulting curve resembles an inverted “horse shoe”.

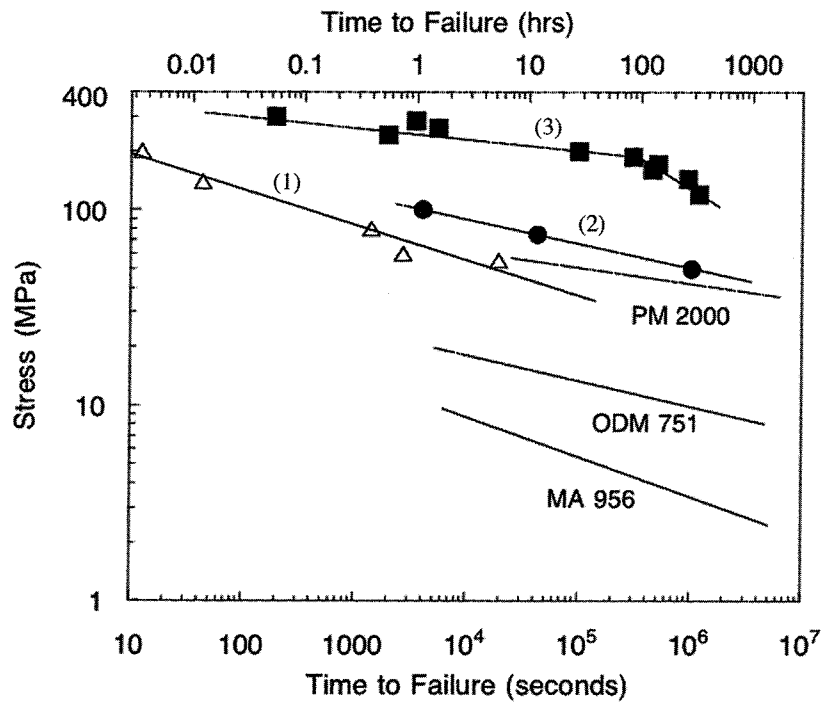


Figure 22.34 Plot of Stress (MPa) versus Time-to-Rupture for Tests Conducted in Air at 1200°C for: (1) 2-D, PW, CG-Nicalon™/CVI-SiC [89]. (2) 2-D, 8HSW, Nextel™720/AS [124]. (3) 3-D Tyranno Lox-M/C/Si-Ti-C-O [153]. For Comparative Purposes, Data are Provided for PM2000, MA 956 and ODM 751 at 1100°C in Air.

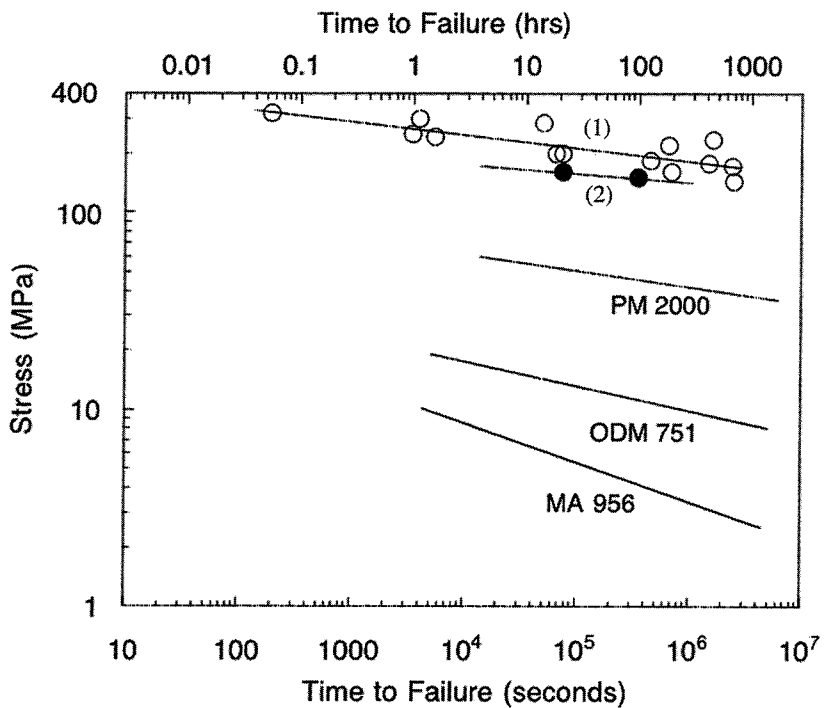


Figure 22.35 Plot of Stress versus Time-to-Rupture for Tests Conducted in Air at 1100°C for: (1) 3-D Tyranno Lox-M/C/Si-Ti-C-O [153]. (2) 2-D, 8HSW, Nextel™720/AS [115]. For Comparative Purposes, Data for PM2000, MA 956 and ODM 751 at 1100°C in Air.

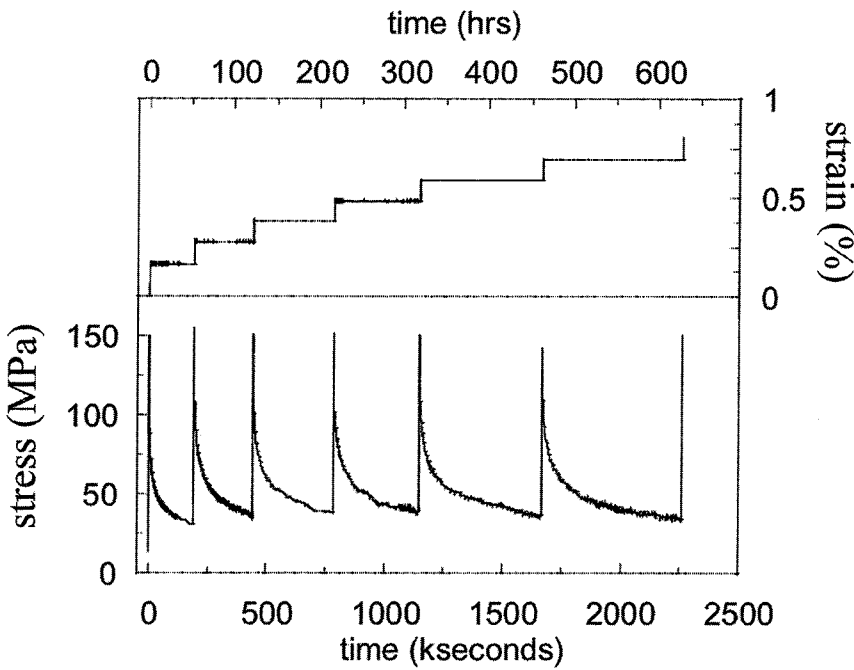


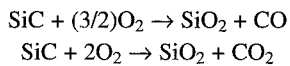
Figure 22.36 Stress-Relaxation Behavior of Sylramic®/PIP-SiNCO CFCC at 1300°C in Air after Successive Straining at Increasingly Larger Strain Levels

applied strain. The relaxation of stress in CFCCs at elevated temperatures is related to viscous deformation of the composite constituents as well as to damage resulting from the application of strain. In the case of C/Mi-SiC CFCCs in air at 1000°C, when the environment can ingress to the interior of the material, stress relaxation results from the oxidation and failure of the reinforcing fibers (Figure 22.37) [123].

ENVIRONMENTAL EFFECTS ON PHYSICAL AND MECHANICAL PROPERTIES

Oxidation and Corrosion

One of the properties that make SiC attractive for applications in air at elevated temperatures is its excellent resistance to oxidation. The mechanism of passive oxidation of SiC is based on the formation of a protective layer of silica according to the following reactions:



The oxidation behavior of SiC-matrix CFCCs in air has been analyzed extensively and values have been reported for the parabolic rate constant as a function of temperature [155–162]. However, despite the remarkable resistance of CVI-SiC to oxidation (in air) at elevated temperatures and ambient pressure, there are certain conditions of stress and temperature for which CVI-SiC matrix CFCCs exhibit severe degradation of mechanical properties as a result of oxidation.

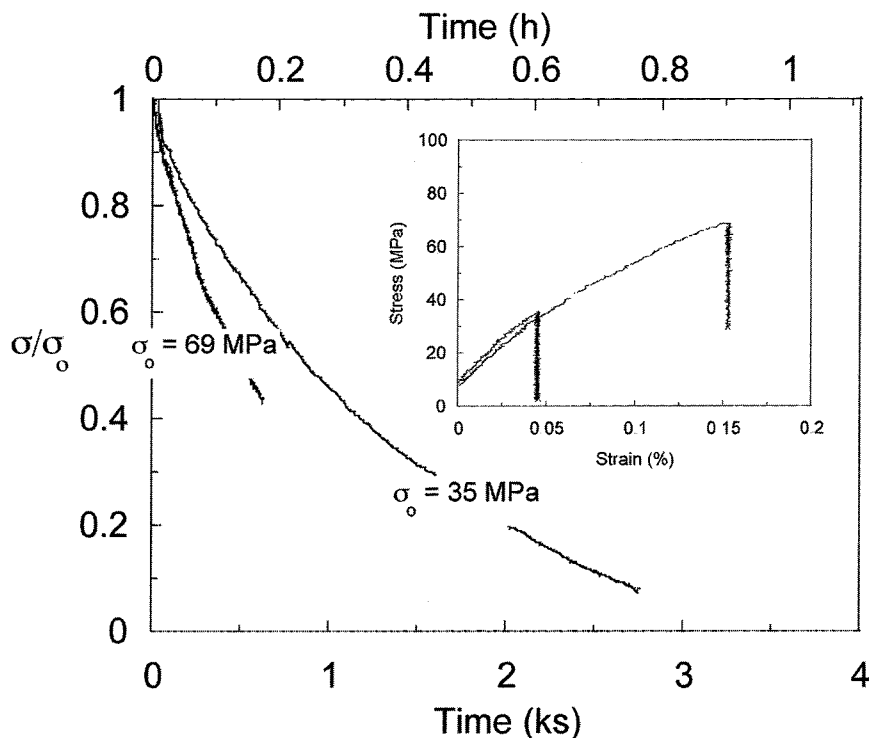


Figure 22.37 Stress-Relaxation Behavior of C/Mi-SiC CFCC at 1000°C in Air at Two Different Initial Stresses. The Inset Shows the Corresponding Stress-Strain Curves [123].

The degradation of the physical and mechanical properties of continuous fiber-reinforced CVI-SiC composites as a result of oxidation, results from the ingress of the environment to the interior of the composite through matrix cracks, open machined surfaces, and fiber ends [88]. For carbonaceous fiber coatings, oxidation results in the removal of the fiber coating, leaving a gap between the fibers and the matrix that will result in the local redistribution of stresses, because load is transferred between the fibers and the matrix through the fiber coating. Once the fibers are exposed to the environment, the fibers will oxidize (in the case of non-oxide) and lead to loss of fiber strength.

Thermokinetic chemical analyses have been formulated to model the oxidation behavior of SiC-based and carbon fiber-reinforced CVI-SiC matrix CFCCs [158,159,160–162]. These analyses, which have been formulated taking into consideration the effect of partial pressures of oxygen and temperature, have provided the thickness of the fiber coating that is critical to promote the sealing of channels, created by the removal of the fiber coating, by matrix oxidation.

To assess the environmental durability of CFCCs in a particular application, it is necessary to evaluate candidate materials under conditions that are as realistic as possible. For example, data available from the evaluation of non-oxide CFCCs in air would not have predicted the degradation that these materials would experience in combustor rigs or actual engine operation [163–167]. In combustion environments water is present in amounts related to the composition of the fuel. In the case of Si-based CFCCs, water vapor will react with silica resulting in accelerated oxidation [165–167]. Chapter 26 presents a detailed discussion of environmental effects on the properties of monolithic ceramics and CFCCs. As a result of the interaction between SiC-based CFCCs and combustion environments, several environmental barrier coating concepts have been developed to protect CFCCs in combustion environments [168–172].

In marine environments, gas turbine components are subjected to even more severe conditions due to the presence of alkalis, which are known to attack SiC [173, 174].

COMPONENTS AND SPECIAL CONFIGURATIONS

To validate methodologies for designing components with CFCCs, it is necessary to proof-test or evaluate entire components, or sections of components, under loading conditions that are representative of those that are expected during service. Scaled combustor liners of CG-NicalonTM/PIP-SiNCO have been evaluated and their properties compared to those of standardized test specimens of the same material [175]. The scaled combustor liner, which was 145 mm in diameter, 2.87 mm in wall thickness and 12.75 mm tall, was subjected to internal pressurization using an elastomeric insert. The scaled combustor liner consisted of a convoluted structure in which segments of CFCC with 8HSW fiber architecture were overlapped at regular angles around the circumference. Figure 22.38 presents tensile stress-strain curves obtained from the evaluation of an ASTM C1275-size test coupon of the same material. Also included in that plot is the hoop stress versus hoop strain curve obtained from the internal pressurization of the scaled liner section. Although the proportional stress limit and the elastic modulus that were obtained from both tests are the same, the ultimate strength is not. This discrepancy results from the fact that the scaled combustor liner failed at a matrix-rich joint region, which would be equivalent to the weldment in a metallic cylindrical structure. Additional variations between results obtained from the evaluation of standardized test specimens and larger components would result from volumetric effects [84,85], from edge effects and constraints or from multiaxial states of stress not reproduced during the evaluation of standardized test specimens.

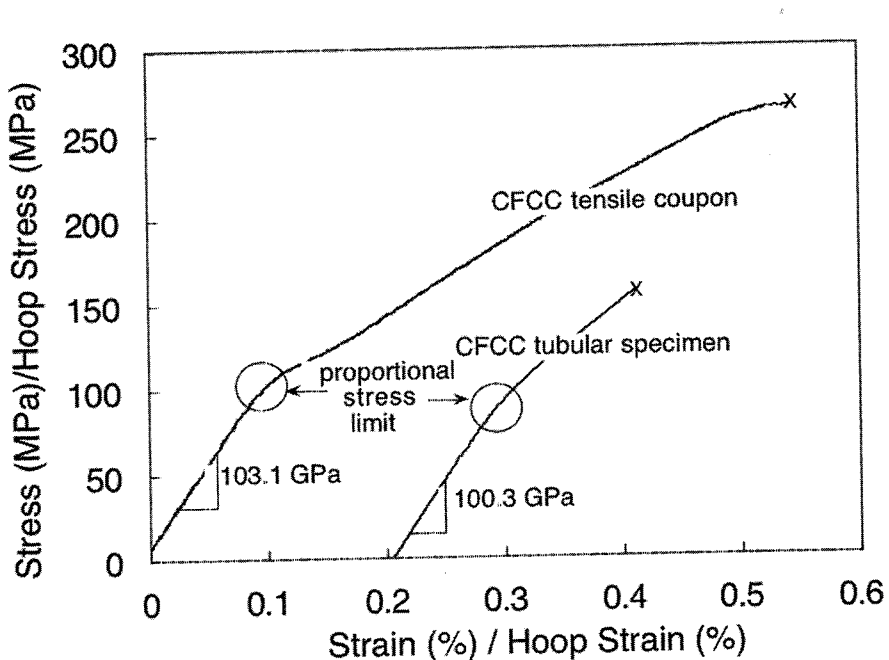


Figure 22.38 Tensile Stress-Strain Behavior of CG-NicalonTM/BN/PIP-SiNCO CFCC Test Coupon (200 mm Long with a Gauge Section 50 mm Long) and Tensile Hoop Stress-Hoop Strain Behavior of CG-NicalonTM/BN/PIP-SiNCO CFCC Tubular Specimen 145 mm Inner Diameter, 2.87 mm Thick and 12.75 mm Tall [175].

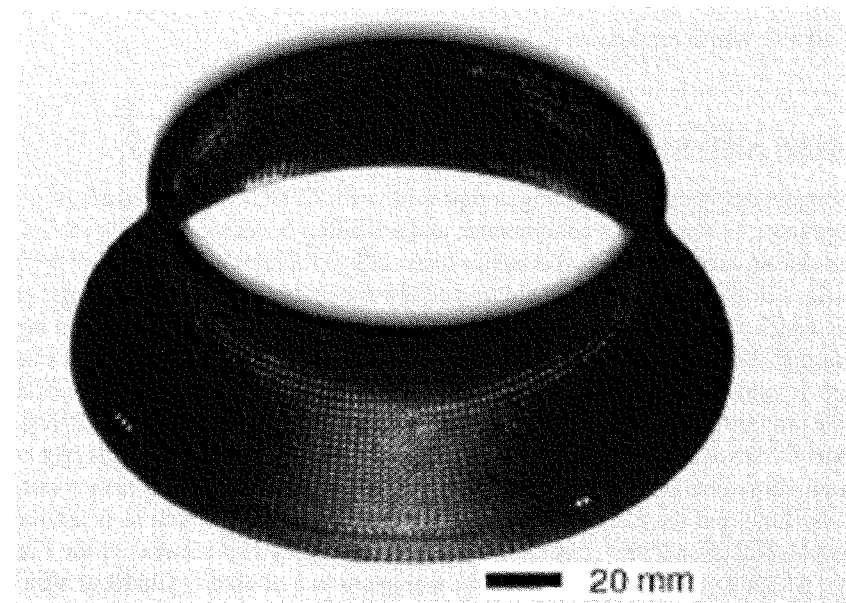
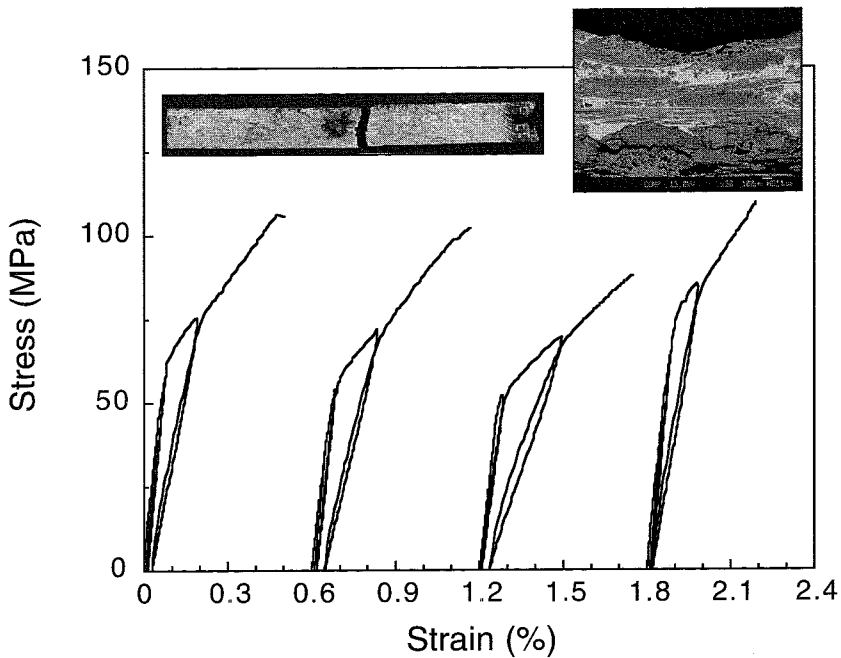


Figure 22.39 CG-Nicalon™/Si-N-C-O CFCC Inner Scroll Support of 100kW Automotive Ceramic Gas Turbine Development Project (Reprinted with permission from ref. [176])

A CG-NicalonTM/SiNCO CFCC inner scroll support for a 100 kW automotive ceramic gas turbine was evaluated by internal pressurization using oil, and instrumented with strain gauges to determine the distribution of strains during the test (Figure 22.39). The CFCC inner scroll support was subjected to increasingly larger values of internal pressure until failure, which occurred at a tangential stress of 180 MPa. The evaluation of tensile test specimens of the same material yielded lower tensile strengths [176] and these discrepancies suggest differences in the structure of the material between test specimen and inner scroll support and errors in the determination of stresses in the latter during pressurization.

In contrast to the applications illustrated above, where the state of stress is relatively simple, in other applications components will be subjected to multiaxial states of stress. This in turn will require the evaluation of special test specimen configurations including the evaluation of components under actual and simulated conditions to develop failure maps and multiaxial strength criteria [94].

One important aspect of the methodology for designing with CFCCs and validating life prediction models consists in determining the residual properties of components. Ideally it would be desirable to use non-destructive techniques that could provide a measure of residual properties as a function of the service history of the component. In the case of combustor liners, their residual mechanical properties (e.g. – tensile stress-strain behavior, interlaminar properties) have been determined after being removed from service operation. Figure 22.40 shows a plot containing stress-strain curves from the tensile evaluation of axial strips of Hi-Nicalon/BN/MI-SiC obtained from combustor liners that had accumulated 13,000+ hours at a peak service temperature of 1260°C [164]. The insets correspond to a photograph of one of those strips, illustrating the degree of corrosion experienced by the material, and a micrograph of a typical cross-sectional area. The stress values in the curves in Figure 22.40 were determined using the overall dimensions of the CFCC, including the thick oxide products. However, when the stresses are computed using the effective remaining cross-sectional area of the CFCC it is found that it only experienced a small loss of strength and most importantly, the CFCC still exhibited composite-like behavior and adequate failure strain comparable to that of the material in the as-processed condition.



**Figure 22.40 Tensile Stress-Strain Curves for Tyranno™-SA/BN/MI-SiC CFCC Strips
Obtained from a Combustor Liner after 13,000+ Hours of Operation. The Insets Correspond to a Photograph of One of Those Strips Illustrating the Amount of Oxidation, and a Micrograph of the Cross-Sectional Area of the Material (Reprinted with permission of K.L. More, Oak Ridge National Laboratory).**

SUMMARY

CFCCs exhibit remarkable physical and mechanical properties and the ability to alleviate elastic stress concentrations at holes and notches by redistributing stresses through various inelastic deformation mechanisms, which are attractive for the manufacture of components for gas turbines and many other industrial applications. CFCCs and their constituents have undergone substantial and significant developments over the last 25 years particularly in the area of reinforcing fibers and matrices. CFCCs currently available exhibit high tensile strength, damage tolerance, exceptional strength retention at elevated temperatures, and resistance to creep and stress-rupture at temperatures as high as 1300°C. Additional work is still needed to address the susceptibility of non-oxide CFCCs to environmental attack in combustion-related environments. Although developments in the area of EBCs are encouraging, dependence on their use does impact the cost and reliability of CFCCs.

All-oxide CFCCs have experienced rapid developments in recent years. There are currently various all-oxide CFCC systems available, which exhibit good mechanical properties and excellent damage tolerance and resistance to stress-rupture and mechanical fatigue. Although their use is currently limited by the microstructural stability of polycrystalline oxide fibers up to 1100°C, efforts are currently under way to develop small-diameter polycrystalline fibers with improved creep resistance and stability at high-temperatures [177].

The need to continue improving the efficiency of power generation systems and industrial processes and meeting increasingly more stringent environmental regulations on emissions remains the driving force for the further development and implementation of CFCCs in upcoming years.

ACKNOWLEDGEMENTS

The author gratefully acknowledges the support of the U.S. Department of Energy through various research programs at Oak Ridge National Laboratory. The support of program managers Debbie Haught, Merrill Smith and Mike Karnitz is sincerely appreciated. The author wishes to thank all those whose work has provided the material for this book chapter. Unless otherwise indicated all figures and tables were provided by the author.

NOMENCLATURE

Al_2O_3	aluminum oxide
AS	aluminosilicate
BN	boron nitride
C	carbon
CFCC	continuous fiber-reinforced ceramic matrix composites
CG	ceramic grade
CGT	ceramic gas turbine
CMC	ceramic matrix composite
CT	compact tension
CVD	chemical vapor deposition
CVI	chemical vapor infiltration
CO	carbon monoxide
DNS	double-notched shear specimen
HSW	harness satin weave
ILSS	interlaminar shear strength
kW	kilowatt
MI	melt infiltrated
ML	multilayer
MW	megawatt
N	nitrogen
NOx	nitrogen oxides
PIP	polymer infiltration and pyrolysis
PW	plain weave
SENB	single edge notch beam
SENT	single edge notch tensile
Si	silicon
SiC	silicon carbide
Si_3N_4	silicon nitride
SiNCO	silicon oxy-carbide-nitride
σ_{PL}	proportional limit stress
TIT	turbine inlet temperature
v_f	fiber volume fraction

REFERENCES

- [1] *Ceramic Fibers and Coatings, Advanced Materials for the 21st Century*, The National Academy of Sciences Press, Washington, D.C., 1998.
- [2] Miller, S., "Advanced Materials Mean Advanced Engines," Mater. World, 4[8], 446–449, 1996.

- [3] Kerans, R. J., Hay, R. S., Parthasarathy, T. A., and Cinibulk, M. K., "Interface Design for Oxidation-Resistant Ceramic Composites," *J. Am. Ceram. Soc.*, 85[11], 2599–2632, 2002.
- [4] Levi, C. G., Zok, F. W., Yang, J-Y, Mattoni, M. and Lofvander, J. P. A., "Microstructural Design of Stable Porous Matrices for All-Oxide Ceramic Composites," *Z. Metallkd.*, 90, 1037–1047, 1999.
- [5] Lewis, M.H., Tye, A., Butler, E., and Al-Dawery, I., "Development of Interfaces in Oxide Matrix Composites," *Key Engineering Materials*, 164[16], 351–356, 1998.
- [6] Tressler, R. E. and Pysher, D. J., "Mechanical Behaviour of High Strength Ceramic Fibres at High Temperatures," *Proc. Satellite Symp. Advanced Structural Inorganic Composites, 7th Int.Meeting on Modern Ceramics Technologies*, Montecatini Terme, Italy, June 27–30, 1990, Materials Science Monographs, 68, Elsevier Science Publishing Co. Inc., Amsterdam, The Netherlands, 1990. pp. 3–18.
- [7] Wilson, D. M., Lieder, S. L., and Lueneburg, D. C., "Microstructure and High Temperature Properties of Nextel 720 Fibers," *Ceram. Eng. and Sci. Proc.*, 16[5], 1005–1014, 1995.
- [8] Milz, C., Goering, J., and Schneider, H., "Mechanical and Microstructural Properties of Nextel 720 Relating to its Suitability for High Temperature Application in CMCs," *Ceram. Eng. and Sci. Proc.*, 20[3], 191–198, 1999.
- [9] Goering, J., Kanka, B., Steinhauser, U., and Schneider, H., "Thermal Barrier Coated Nextel 720 Fiber/Mullite Matrix Composites: Their Potential for Long-term High Temperature Use in Gas Turbines," *Ceram. Eng. and Sci. Proc.*, 21[3], 613–618, 2000.
- [10] Lara-Curcio E. and More, K. L., "Stress-Rupture of NextelTM 720 Fiber-Reinforced Aluminosilicate Composites: The Role of Microstructural Evolution," presented at the 24th Annual Cocoa Beach Conference and Exposition, Cocoa Beach, FL, USA, January 25, 2000.
- [11] *Handbook on Continuous Fiber-Reinforced Ceramic Matrix Composites*, Lehman, R. L., El-Rahaiby, S. K., and Wachtman, J. B., eds., The American Ceramic Society, Westerville, OH, USA, 1995.
- [12] Lackey, W.J. and Starr, T.L., "Composites by Chemical Vapor Infiltration: Processing, Structure and Properties," in *Fiber Reinforced Ceramic Composites: Materials Processing and Technology*, Mazdiyasni, K. S., ed., Materials Science and Process Technology Series, Noyes Publications, Park Ridge, NJ, USA, 1990. pp. 397–450.
- [13] Clarke, D.A., "Fabrication Aspects of Glass Matrix Composites for Gas Turbine Applications," in *New Materials and their Applications*, University of Warwick, UK, 10–12 Apr. 1990, IOP Publishing, IOP Redcliffe Way, Bristol BS1 6NX, UK, 1990. pp. 173–183.
- [14] Dominy, J., "Structural Composites in Civil Gas Turbine Aero Engines," *Compos. Manuf. (UK)*, 5[2], 69–72, June 1994.
- [15] Dominy, J., Evans, W. J., and Duff, S. L., "Ceramics in Aero Gas Turbines. An Engineer's View," *Materials Congress '98, Frontiers in Materials Science and Technology*, Cirencester, UK, 6–8 April 1998, Institute of Materials, Materials for High Power Generation and Process Plant Applications, UK, 2000. pp. 335–343.
- [16] Ruffles, C., "Applications of Advanced Composites in Gas Turbine Aero Engines," *ICCM/9. Metal Matrix Composites. Vol. I*, Madrid, Spain, July 12–16, 1993. pp. 123–130.
- [17] Bennett, A., "Overview of the Advanced Ceramics for Turbines (ACT) Programme," *Advanced Materials Journal*, 1[3], 21–22, 1990.
- [18] Beesley, C. P., "Application of CMCs in High Integrity Gas Turbine Engines," *Key Engineering Materials*, 127–131, Part 1, 165–174, 1997.

- [19] Nardone, V. C., and Prewo, K. M., "Tensile Performance of Carbon Fiber-Reinforced Glass," *J. Mater. Sci.*, 23, 168–180, 1988.
- [20] Karnitz, M. A., Craig, D. F., and Richlen, S., L., "Continuous Fiber Ceramic Composites Program," *Am. Ceram. Soc. Bull.*, 70[3], 430–435, 1991.
- [21] van Roode, M., Brentnall, W.D., Norton, P.F., and Boyd, G.L., "Ceramic Stationary Gas Turbine Development Program—First Annual Summary," ASME paper 94-GT-313, presented at the International Gas Turbine and Aeroengine Congress and Exposition, The Hague, The Netherlands, June 13–16, 1994.
- [22] Brewer, D., "HSR/EPM Combustor Materials Development Program," *Materials Science and Engineering A*, 261[1–2], 284–291, 1999.
- [23] DiCarlo, J.A., Yun, H. M., Morscher G. N., and Ogbuji, L. U. T., "Progress in SiC/SiC Composites for Engine Applications," in *High Temperature Ceramic Matrix Composites*, Krenkel, W., Naslain R., and Schneider, H., eds., 4th International Conference on High Temperature Ceramic Matrix Composites (HT-CMC4), Munich, Germany October 1–3, 2001, Wiley-VCH, 2001, pp. 777–782.
- [24] Chung, V., Balis, C., Sohi, M., and van Erp, C., "Ceramic Matrix Composite Materials in Advanced Manned Gas Turbine Engine Combustors," in *Processing, Fabrication & Application of Advanced Composites*, Long Beach, California, USA, 9–11 Aug. 1993, ASM International (USA), 1993, pp. 91–97.
- [25] Stephens, J. R., "Intermetallic and Ceramic Matrix Composites for 815–1370°C (1500–2500°F) Gas Turbine Engine Applications," NASA Tech. Memo., NASA TM-102326, *The Status of NASA's Advanced High Temperature Engine Materials Technology Program (HITEMP)*, 1990, p.9.
- [26] Levine, S.R., *Ceramic Composites—Enabling Aerospace Materials*, NASA TM 105599 (1992) for paper presented at the 37th International Gas Turbine and Aeroengine Congress and Exposition, Cologne, Germany, June 1–4, 1992.
- [27] Lamicq, P. J., and Jamet, J. F., "Thermostructural CMCs: An Overview of the French Experience," *Ceramic Transactions*, 57, 1–12, 1995.
- [28] Spiet, P. and Habarou, G., "Applications of Continuous Fibre Reinforced Ceramic Composites in Military Turbojet Engines," in *Proceedings of the 5th Conference and Exhibition of the European Ceramic Society (ECERS V)*, P. Abelard, J. Baxter, D. Bortzmeyer, et al., eds., Versailles, France, June 22–26, 1997, Key Engineering Materials, 132–136[3], 1930–1933, 1997.
- [29] Terpstra, R. A., Gubbels, F., Roman, Y., van der Heijde, H., and Brinkman, E., "Ceramic Components in Gas Turbines," *Klei/Glas/Keram.*, 17[6/7], 14–15, 1996.
- [30] Gubbels, G. H. M., van der Heijde, J. C. T., Brinkman, H. W., Linden, J. L., and Terpstra, R. A., "Development of Ceramic Components for Gas Turbine Application," in *Proceedings of the 5th Conference and Exhibition of the European Ceramic Society (ECERS V)*, P. Abelard, J. Baxter, D. Bortzmeyer, et al., eds., Versailles, France, June 22–26, 1997, Key Engineering Materials, 132–136[3], 2096–2099, 1997.
- [31] Iffländer, K., Gualco, G. C., Rosatelli, F., Hampshire, S., Van Brug, E. H., Ferrière, A., Rodriguez, G. P., Fordham, R. J., Dupel, P., Mason, N., and Nedele, M., "Selective Material Characterization of Ceramic Matrix Composites for Advanced Gas Turbines," *Ceram. Eng. and Sci. Proc.*, 18[3], 625–632, 1997.
- [32] Kaya, H., "The Application of Ceramic-Matrix Composites to the Automotive Ceramic Gas Turbine," *Composites Science and Technology*, 59, 861–872, 1999.

- [33] Nishio, K., Igashira, K. I., Take, K., and Suemitsu, T., "Development of a Combustor Liner Composed of Ceramic Matrix Composite (CMC)," *Transactions of the ASME, Journal of Engineering for Gas Turbines and Power*, 121[1], 12–17, 1999.
- [34] Nishio, K., Igashira, K., and Suemitsu, T., "Applications of SiC/SiC to the Components of a Gas Turbine," *Ceram. Jap.*, 34[4], 286–288, 1999.
- [35] Kohyama, A. and Katoh, Y., "Overview of CREST-ACE Program for SiC/SiC Ceramic Composites and their Energy System Applications," *Ceramic Transactions*, 144, 3–18, 2002.
- [36] Smith, K.O. and Fahme, A., "Experimental Assessment of the Emissions Benefits of a Ceramic Gas Turbine Combustor," ASME paper 96-GT-318, presented at the International Gas Turbine and Aeroengine Congress and Exposition, Birmingham, England, U.K., June 10–13, 1996.
- [37] Corman, G., and Luthra, K., "Improved Properties of Gas Turbine Engine Components Utilizing CFCC and Melt Infiltration," *Ind. Heat*, 63[12], 39–40, 1996.
- [38] Corman, G.S., Brun, M.K., and Luthra, K.L., "SiC Fiber Reinforced SiC-Si Matrix Composites Prepared by Melt Infiltration (MI) for Gas Turbine Engine Applications," ASME paper 99-GT-234, presented at the International Gas Turbine and Aeroengine Congress and Exposition, Indianapolis, IN, USA, June 7–10, 1999.
- [39] Price, J., Jimenez, O., Parthasarathy, V., Miriyala, N., and Leroux, D., "Ceramic Stationary Gas Turbine Development Program—Seventh Annual Summary," ASME Paper 2000-GT-0075, presented at the ASME TURBO EXPO, Land, Sea & Air 2000, Munich, Germany, May 8–11, 2000.
- [40] Simpson, J. F., Parthasarathy, V. M., Fahme, A., "Testing of Monolithic Ceramics and Fiber Reinforced Ceramic Composites for Gas Turbine Combustors," *Ceram. Eng. and Sci. Proc.*, 18[4], 229–236, 1997.
- [41] Fohey, W. R., Battison, J. M., Nielsen, T. A., and Hastings, S., "Ceramic Composite Turbine Engine Component Evaluation," *Ceram. Eng. and Sci. Proc.*, 16[4], 459–466, 1995.
- [42] Kameda, T., Sayano, A., Amiji, N., Ichikawa, H., Hamada, H., Fujita, A., and Uozumi, T., "Fabrication and Mechanical Properties of Reaction Sintered Silicon Carbide Matrix Composite," *Ceram. Eng. and Sci. Proc.*, 18[3], 419–426, 1997.
- [43] Matsumoto, M., Fujioka, N., Hayakawa, T., Kawamura, N., and Sato, K., "Development of a Combustion Chamber Liner Utilizing a Long-Fiber Reinforced Composite Material Made Using the Polysilazane Impregnation Method and the Chemical Vapor Deposition Method," *Key Engineering Materials*, 164, 49–52, 1998.
- [44] Itoh, Y., Kameda, T., Suyama, S., Nishida, K., and Okamura, T., "Development of Continuous Fiber Reinforced Reaction Sintered Silicon Carbide Matrix Composite and Fabrication of Gas Turbine Hot Parts," *Materia Japan*, 39[1], 63–65, 2000.
- [45] Holmquist, M., Sudre, O., Lundberg, R., Molliex, L., Razzell, T., and Adlerborn, J., "Development of Ultra High Temperature Ceramic Composites for Gas Turbine Combustors," ASME paper 97-GT-413, presented at the 42nd International Gas Turbine & Aeroengine Congress & Exposition, Orlando, FL, USA, June 2–5, 1997.
- [46] Holmquist M., Lundberg, R., Sudre, O., Razzell, A. G., Molliex, L., Benoit, J., and Adlerborn, J., "Alumina/Alumina Composite with a Porous Zirconia Interphase. Processing, Properties and Component Testing," *J. Eur. Ceram. Soc.*, 20, 599–606, 2000. © 2000, Elsevier, All rights reserved.
- [47] Sudre, O., Razzell, A. G., Molliex, L., and Holmquist, M., "Alumina Single-Crystal Fiber Reinforced Alumina Matrix For Combustor Tiles," *Ceram. Eng. and Sci. Proc.*, 19[4], 273–280, 1998.

- [48] Razzell, A. G., Molliex, L., Holmquist, M., and Sudre, O., "Oxide/Oxide Ceramic Matrix Composites in Gas Turbine Combustors," ASME paper 98-GT-30, presented at the ASME International Gas Turbine and Aeroengine Congress and Exhibition, Stockholm, Sweden, June 2–5, 1998.
- [49] Filsinger, D., Münz, S., Schulz, A., Wittig, S., and Andrees, G., "Experimental Assessment of Fiber Reinforced Ceramics for Combustor Walls," ASME paper 97-GT-154, presented at the 42nd International Gas Turbine & Aeroengine Congress & Exposition, Orlando, FL, USA, June 2–5, 1997.
- [50] Zawada, L. P. and Lee, S. S., "Evaluation of Four CMCs for Aerospace Turbine Engine Divergent Flaps and Seals," *Ceram. Eng. and Sci. Proc.*, 16[4], 337–339, 1995.
- [51] Staehler, J.M. and Zawada, L.P., "Performance of Four Ceramic-Matrix Composite Divergent Flap Inserts Following Ground Testing on an F110 Turbofan Engine," *J. Am. Ceram. Soc.*, 83[7], 1727–1738, 2000.
- [52] Das, S., Harlan, N., Lee, G., Beaman, J.J., Bourell, D.L., Barlow, J.W., Fuesting, T., Brown, L., and Sargent, K., "Direct SLS Processing for Production of Cermet Composite Turbine Sealing Components," *Mater. Manuf. Processes*, 13[2], 241–261, 1998.
- [53] Morrison, J. A. and Kauth, K. M., "Design and Analysis of a CMC Turbine Blade Tip Seal for a Land-based Power Turbine," *Ceram. Eng. and Sci. Proc.*, 19[4], 249–256, 1998.
- [54] Khandelwal, P., Shepard, S. M., and Ahmed, T., "Thermal Wave Nondestructive Evaluation of Ceramic Matrix Composite Components," *Ceram. Eng. and Sci. Proc.*, 18[4], 425–433, 1997.
- [55] Jarmon, D. C. and Prewo, K. M., "Rotor for a Gas Turbine Engine," US Patent Number 4808076, 28 Feb. 1989.
- [56] Huynh, T., Burkland, C. V., and Bustamante, B., "Densification of a Thick Disk Preform with Silicon Carbide Matrix by CVI," *Ceram. Eng. and Sci. Proc.*, 12[9–10], 2005–2014, 1991.
- [57] Klacka, R. W., Headinger, M. H., Moschelle, W. R., and Farr, J. D., *C/SiC Turbine Rotor Development*, NASA Conference Publication No. 3235, Pt. 2, 1994. pp. 855–862.
- [58] Natsumura, T., Nojima, Y., Suzumura, N., Araki, T., Moriya, K., and Yasuhira, K., "Component Design of CMC and MMC Rotor for Turbine Engine Applications," in *Advanced Materials & Processes: Preparing for the New Millennium*, Society for the Advancement of Material and Process Engineering, USA, Oct. 1999. pp. 130–141.
- [59] Okura, A., Tanatsugu, N., Naruo, Y., and Tachibana, M., "On the Test of C/C Composite Turbine Blade," *Advanced Composites '93: International Conference on Advanced Composite Materials*, Wollongong, Australia, Feb 15–19, 1993, The Minerals, Metals & Materials Society, USA, 1993. pp. 147–153.
- [60] Araki, T., Suzumura, N., Masaki, S., Natsumura, T., Onozuka, M., Ohnabe, H., and Yasuhira, K., "Manufacturing of Ceramic Matrix Composite Rotor for Advanced Gas-Generator," *Ceram. Eng. and Sci. Proc.*, 19[4], 241–248, 1998.
- [61] Sanokawa, Y., Ido, Y., Sohda, Y., Nakazawa, N., and Kaya, H., "Application of Continuous Fiber Reinforced Silicon Carbide Matrix Composites to a Ceramic Gas Turbine Model for Automobiles," *Ceram. Eng. and Sci. Proc.*, 18[4], 221–228, 1997.
- [62] DiMascio, P. S., Orenstein, R. M., Schroder, M. S., Tognarelli, L., Corman, G. S., and Dean, A. J., Chapter 9 in *Ceramic Gas Turbine Design and Test Experience, Progress in Ceramic Gas Turbine Development, Volume I*, van Roode, M., Ferber, M. K., and Richerson, D. W., eds., ASME Press, New York, NY, USA, 2002. pp. 225–236.

- [63] *The 9th International Symposium on Ultra-high Temperature Materials '99*, Japan Ultra-high Temperature Materials Research Center, Tajimi City, Japan, 1999.
- [64] Lara-Curzio, E. and Jenkins, M. G., "Development of Test Standards for CFCCs in the US," *Composites Part A*, 30[4], 561–567, 1999.
- [65] Lara-Curzio, E., "Status of Standardization Activities for Ceramic Matrix Composites in the United States," *Ceramic Transactions*, 144, 191–206, 2002.
- [66] Mizuno, M., Cao J-W., Nagano, Y., and Kaya, H., "Development On Standard Test Methods For Ceramic Matrix Composites," *Ceram. Eng. and Sci. Proc.*, 19[3], 541–548, 1998.
- [67] Lara-Curzio, E., in "Continuous Fiber Ceramic Composite Program Task 2: Supporting Technologies," in *Bimonthly Progress Report for October-November 1994*, Oak Ridge National Laboratory, Oak Ridge, TN, USA, 1994. pp. 25–30.
- [68] Evans, A. G., Zok, F. W., and Mackin, T. J., "The Structural Performance of Ceramic Matrix Composites," in *High Temperature Mechanical Behavior of Ceramic Composites*, Nair, S. V. and Jakus, K., eds., Butterworth-Heinemann, Newton, MA, USA, 1995. pp. 3–86.
- [69] Huger, M., Fargeot, D., and Gault, C., "Ultrasonic Characterization of Oxidation Mechanisms in Nicalon/C /SiC Composites," *J. Am. Ceram. Soc.*, 77[10], 2554–2560, 1994.
- [70] Sakata, M. and Ohnabe, H., "Measurement of Orthotropic Elastic Constants of Ceramic Matrix Composite from Impact Sound," in *Thermal and Mechanical Test Methods and Behavior of Continuous-Fiber Ceramic Composites, ASTM STP 1309*, Jenkins, M. G., Gonczy, S. T., Lara-Curzio, E., Ashbaugh, N. E., and Zawada, L. P., eds., American Society for Testing and Materials, West Conshohocken, PA, USA, 1997. pp. 291–305.
- [71] Camus, G., El Bouazzaoui, R., and Baste, S., "Development of Damage in a 2D Woven C/SiC Composite Under Mechanical Loading. II. Ultrasonic Characterization," *Composites Science and Technology*, 56[12], 1373–1382, 1996.
- [72] Camus, G., Guillaumat, L., and Baste, S., "Development of Damage in a 2D Woven C/SiC Composite Under Mechanical Loading. I. Mechanical Characterization," *Composites Science and Technology*, 56[12], 1363–1372, 1996.
- [73] Liaw, P. K., Yu, N., Hsu, D. K., Miriyala, N., Saini, V., Snead, L. L., McHargue, C. J., and Lowden, R. A., "Moduli Determination of Continuous Fiber Ceramic Composites (CFCCs)," *J. Nucl. Mater.*, 219[1–3], 93–100, March 1995.
- [74] Camus, G. and Barbier, J. E., "Tensile Behavior of a 2D Woven C/SiC Composite at Ambient and Elevated Temperatures," *Ceramic Transactions*, 57, 407–412, 1995.
- [75] Steffier, W. S., "The Orthotropic Mechanical Behavior of Nicalon® Fiber-Reinforced SiC-Matrix Composites," *Ceram. Eng. and Sci. Proc.*, 14[9–10], 1045–1057, 1993.
- [76] Chulya, A., Gyekenyesi, J. Z., and Gyekenyesi, J. P., "Failure Mechanisms of 3-D Woven SiC/SiC Composites Under Tensile and Flexural Loading at Room and Elevated Temperatures," *Ceram. Eng. and Sci. Proc.*, 13[7–8], 420–432, 1992.
- [77] *Data Sheet*, Allied Signal Composites, Inc., Newark, DE, USA.
- [78] Wurtinger, H. and Mühlratzer, A., "Cost Effective Manufacturing Methods for Structural Ceramic Matrix Composite (CMC) Components," ASME Paper 96-GT-296, presented at the 1996 International Gas Turbine and Aeroengine Congress and Exhibition, Birmingham, UK, June 10–13, 1996.
- [79] Heathcote, J. A., Gong, X-J., Yang, J. Y., Ramamurty, U., and Zok, F. W., "In-Plane Mechanical Properties of an All-Oxide Ceramic Composite," *J. Am. Ceram. Soc.*, 82[10], 2721–2730, 1999.

- [80] Jenkins, M. G., Lara-Curzio, E., Gonczy, S. T., and Zawada, L. P., "Multiple-Laboratory Round-Robin Study of the Flexural, Shear and Tensile Behavior of a Two-Dimensionally Woven NicalonTM/SylramicTM Ceramic Matrix Composite," in *Mechanical, Thermal and Environmental Testing and Performance of Ceramic Composites and Components, ASTM STP 1392*, Jenkins, M. G., Lara-Curzio, E., and Gonczy, S. T., eds., American Society for Testing and Materials, West Conshohocken, PA, USA, 2000, pp. 15–30.
- [81] *Data Sheet*, COI Ceramics Inc., San Diego, CA, USA, 2003.
- [82] C1275-00, *Standard Test Method for Monotonic Tensile Behavior of Continuous Fiber-Reinforced Advanced Ceramics with Solid Rectangular Cross-Section Specimens at Ambient Temperatures*, American Society for Testing and Materials, West Conshohocken, PA, USA, 1990.
- [83] Piccola, J. P., Jenkins, M. G., and Lara-Curzio, E., in *Thermal and Mechanical Test Methods and Behavior of Continuous-Fiber Ceramic Composites, ASTM STP 1309*, Jenkins, M. G., Gonczy, S. T., Lara-Curzio, E., Ashbaugh, N. E., and Zawada, L. P., eds., ASTM, West Conshohocken, PA, USA, 1997, pp. 3–15.
- [84] Nozawa, T., Hinoki, T., Katoh, Y., Kohyama, A., and Lara-Curzio, E., "Influence of Specimen Geometry on Tensile Properties of 3-D SiC/SiC Composites," *Ceramic Transactions*, 124, 351–362, 2001.
- [85] Nozawa, T., Katoh, Y., Kohyama, A., and Lara-Curzio, E., "Specimen Size Effect on the In-Plane Shear Properties of SiC/SiC Composites," *Ceramic Transactions*, 139, 127–138, 2002.
- [86] Lacombe, A. and Bonnet, C., "Ceramic Matrix Composites: Key Materials for Future Space Plane Technologies," Paper AIAA-90-5208 presented at the *AIAA Second International Aerospace Planes Conference*, October 29–31, 1990, Orlando, FL, USA.
- [87] Halbig, M. C., Brewer, D. N., Eckel, A. J., and Cawley, J. D., "Stressed Oxidation of C/SiC Composites," *Ceram. Eng. and Sci. Proc.*, 18[3], 547–554, 1997.
- [88] Effinger, M. R., Tucker, D. S., and Barnett, T. R., "Tensile and Interlaminar Shear Evaluation of DuPont Lanxide CMCs," *Ceram. Eng. and Sci. Proc.*, 17[4], 316–323, 1996.
- [89] Choi, S. R. and Gyekenyesi, J. P., "Effect of Load Rate on Tensile Strength of Various CFCCs at Elevated Temperatures—An Approach to Life-Prediction Testing," *Ceram. Eng. and Sci. Proc.*, 22[3], 597–606, 2001.
- [90] Sørensen, B. F. and Holmes, J. W., "Effect of Loading Rate on the Monotonic Tensile Behavior of a Continuous-Fiber-Reinforced Glass-Ceramic Matrix Composite," *J. Am. Ceram. Soc.*, 79[2], 313–320, 1996.
- [91] Lara-Curzio, E., Unpublished Results, 2003.
- [92] Lara-Curzio, E. and C. M. Russ, "On the Matrix Cracking Stress and the Redistribution of Internal Stresses in Brittle-Matrix Composites," *J. Mater. Sci. Eng.*, A250, 270–278, 1998.
- [93] Zawada L. P. and Goecke, K. E., "Testing Methodology for Measuring Transthickness Tensile Strength for Ceramic Matrix Composites," in *Mechanical, Thermal and Environmental Testing of Ceramic Composites and Components, ASTM STP 1392*, Jenkins, M. G., Lara-Curzio, E., and Gonczy, S. T., eds., American Society for Testing and Materials, West Conshohocken, PA, USA, 2000, pp. 62–85.
- [94] Percival, M. J. L., Claxton, E., Gabeltaud, S., Dambrine, B., and Maire, J. F., "Material Testing for Multiaxial Macroscopic Modeling of Ceramic Matrix Composites," *Key Engineering Materials*, 127–131, 791–798, 1997.

- [95] C1468-00, *Standard Test Method for Transthickness Tensile Strength of Continuous Fiber-Reinforced Advanced Ceramics at Ambient Temperature*, ASTM, American Society for Testing and Materials, West Conshohocken, PA, USA, 1990.
- [96] Lara-Curzio, E., and M. G. Jenkins, "Multi-Laboratory Round Robin Study of the Shear Behavior of a Continuous Fiber-Reinforced Ceramic Matrix Composite," presented at the 23rd Annual Cocoa Beach Conference and Exposition, Cocoa Beach, Florida January 28, 1999.
- [97] Lara-Curzio, E., and Boisvert R. P., "Time-Dependent Deformation of Polymer-Derived CFCCs," *CFCC News*, 9, 13–15, August 1997,
- [98] Fang, N. J.-J. and Chou, T.-W., "Characterization of Interlaminar Shear Strength of Ceramic Matrix Composites," *J. Am. Ceram. Soc.*, 76[10], 2539–2548, 1993.
- [99] Lara-Curzio, E. and Singh, M., "High-Temperature Interlaminar Shear Strength of Hi-Nicalon Fiber-Reinforced MI-SiC Matrix Composites with BN/SiC Fiber Coating," *J. Mater. Sci. Letters*, 19, 657, 2000.
- [100] Lara-Curzio, E. and Ferber, M. K., "Shear Strength of Continuous Fiber Reinforced Ceramic Composites," in *Thermal and Mechanical Test Methods and Behavior of Continuous-Fiber Ceramic Composites, ASTM STP 1309*, Jenkins, M. G., Gonczy, S. T., Lara-Curzio, E., Ashbaugh, N. E., and Zawada, L. P., eds., American Society for Testing and Materials, West Conshohocken, PA, USA, 1997. pp. 31–48.
- [101] Mackin, T. J., Purcell, T. E., He, M. Y., and Evans, A. G., "Notch Sensitivity and Stress Redistribution in Three Ceramic-Matrix Composites," *J. Am. Ceram. Soc.*, 78[7], 1719–1728, 1995.
- [102] Gomina, M., Themines, D., Chermant, J. L. and Osterstock, F., "An Energy Evaluation for C/SiC Composite Materials," *International Journal of Fracture*, 34, 219–228, 1987.
- [103] Stull, K. R. and Parviz-Majidi, A., "Fracture Toughness of Fiber-Reinforced Glass-Ceramic and Ceramic Matrix Composites," *Ceram. Eng. and Sci. Proc.*, 12[7–8], 1452–1461, 1991.
- [104] Heraud, L. and Spiet, P., "High-Toughness C/SiC and SiC/SiC in Heat Engines," in *Whisker- and Fiber-Toughened Ceramics*, Bradley, R. A., Clark, D. E., Larsen, D. C. and Stiegler, J. O., eds., ASM International, Oak Ridge, TN, USA, 1988. pp. 217–224.
- [105] Yang, J. M., Lin, W., Shih, C. J., Kai, W., Jeng, S. M., and Burkland, C.U., "Mechanical Behaviour of Chemical Vapour Infiltration-Processed Two- and Three-Dimensional Nicalon/SiC Composites," *J. Mater. Sci.*, 26, 2954–2960, 1991.
- [106] Goto, K. and Kagawa, Y. "Fracture Behavior and Toughness of a Plane-Woven SiC Fiber-Reinforced SiC Matrix Composite," *Materials Science and Engineering A*, 211, 72–81, 1996.
- [107] Xu, Y., Cheng, L., Zhang, L., and Yan, D., "Mechanical Properties and Microstructural Characteristics of Carbon Fiber Reinforced Silicon Carbide Matrix Composites by Chemical Vapor Infiltration," *Key Engineering Materials*, 164–165, 73–76, 1999.
- [108] Shen, J. Y., Hirth, J. P., Zok, F. W., and Heathcote, J. A., "Effect of Notch Root Radius on the Initiation Toughness of a C-fiber/SiC-matrix Composite," *Scripta Materialia*, 38, 15–19, 1998.
- [109] Droillard, C., Voisard, P., Heibst, C., and Lamon, J., "Determination of Fracture Toughness of 2-D Woven SiC Matrix Composites Made by Chemical Vapor Infiltration," *J. Am. Ceram. Soc.* 78[5], 1201–1211, 1995.
- [110] Mizuno, M., Nagano, Y., Usami, H., and Kagawa, Y., "Effect of Specimen Shape on Fracture Toughness and Effective Fracture Energy in SiC-SiC Composite," *Ceram. Eng. and Sci. Proc.*, 15[5], 859–866, 1994.

- [111] Nair, S. V. and Wang, Y. L., "Failure Behavior of a 2-D Woven SiC Fiber/SiC Matrix Composite at Ambient and Elevated Temperatures," *Ceram. Eng. and Sci. Proc.*, 13[7–8], 433–441, 1992.
- [112] Nair, S. V. and Wang, Y. L., "Toughening Behavior of a Two-Dimensional SiC/SiC Woven Composite at Ambient Temperature: I, Damage Initiation and R-Curve Behavior," *J. Am. Ceram. Soc.*, 81[5], 1149–1156, 1998.
- [113] Kramb, V. A., John, R., and Zawada, L. P., "Notched Fracture Behavior of an Oxide/Oxide Ceramic-Matrix Composite," *J. Am. Ceram. Soc.*, 82[11], 3087–3096, 1999.
- [114] Antti M., and Lara-Curzio, E., "Effect of Notches, Specimen Size, and Fiber Orientation on the Monotonic Tensile Behavior of Continuous Fiber-Reinforced Oxide/Oxide Composites at Ambient and Elevated Temperatures," *Ceram. Eng. and Sci. Proc.*, 22[3], 643–650, 2001.
- [115] John, R., Buchanan J. R. and Zawada, L. P., "Notch-Sensitivity of a Woven Oxide/Oxide Ceramic Matrix Composite," in *Mechanical, Thermal and Environmental Testing of Ceramic Composites and Components, ASTM STP 1392*, Jenkins, M. G., Lara-Curzio, E., and Gonczy, S. T., eds., American Society for Testing and Materials, West Conshohocken, PA, USA, 2000. pp. 172–181
- [116] Hasselman, D. P. H. and Donaldson, K. Y., "Thermal Conductivity of Continuous Fiber-Reinforced Ceramic Matrix Composites," in *Handbook on Continuous Fiber-Reinforced Ceramic Matrix Composites*, Lehman, R. L., El-Rahaiby, S. K. and Wachtman, J. B., Eds, The American Ceramic Society, Westerville, OH, USA, 1995. pp. 547–583.
- [117] Youngblood, G. E., Senor, D. J., Jones, R. H., and Graham, S. "The Transverse Thermal Conductivity of 2-D SiC/SiC Composites," *Composites Science and Technology*, 62, 1127–1139, 2002.
- [118] Mital, S. K., Bhatt, R. T., and Murthy, P. L. N., "Influence of Constituents on the Properties of Melt-Infiltrated SiC/SiC Composites," paper AIAA 2002–1686, 2002.
- [119] Beecher, S. C., Dinwiddie, R. B., and Lowden, R. A., "The Thermal Conductivity of Carbon Coated Silicon Carbide Fibers Embedded in a Silicon Carbide Matrix," in *Thermal Conductivity*, Tong, T. T., ed., Technomic Publishing Co., Inc., Tempe, Arizona, USA, 22, 324–334, 1994.
- [120] Snead, L. L. and Schwarz, O. J., "Advanced SiC Composites for Fusion Applications," *Journal of Nuclear Materials*, 219, 3–14, 1995.
- [121] Ahuja, S., Ellingson, W. A., Steckenrider, J. S., and Koch, S. J., "Infrared-Based NDE Methods for Determining Thermal Properties and Defects in Ceramic Composites," in *Thermal and Mechanical Test Methods and Behavior of Continuous-Fiber Ceramic Composites, ASTM STP 1309*, Jenkins, M. G., Gonczy, S. T., Lara-Curzio, E., Ashbaugh, N. E., and Zawada, L. P., eds., American Society for Testing and Materials, West Conshohocken, PA, USA, 1997. pp. 209–218
- [122] Eckel, A. J. and Bradt, R. C., "Thermal Expansion of Laminated, Woven, Continuous Ceramic Fiber /Chemical-Vapor-Infiltrated Silicon Carbide Matrix Composites," *J. Am. Ceram. Soc.* 73[5], 1334–1338, 1990.
- [123] Lara-Curzio, E. and Singh, M., "The Time-Dependent Deformation of Carbon Fiber-Reinforced Melt-Infiltrated Silicon Carbide Matrix Composites: Stress-Rupture and Stress-Relaxation Behavior in Air at 1000°C," in *Mechanical, Thermal and Environmental Testing of Ceramic Composites and Components, ASTM STP 1392*, Jenkins, M. G., Lara-Curzio, E., and Gonczy, S. T., eds., American Society for Testing and Materials, West Conshohocken, PA, USA, 2000. pp. 216–228
- [124] Lara-Curzio, E., "Stress-Rupture, Overstressing and a New Methodology to Assess the High-Temperature Durability and Reliability of CFCCs," in *Mechanical, Thermal and Environmental Testing of Ceramic Composites and Components, ASTM STP 1392*, Jenkins, M. G., Lara-Curzio, E., and Gonczy, S. T., eds., American Society for Testing and Materials, West Conshohocken, PA, USA, 2000. pp. 107–117

- [125] Eckel, A. J., Herbell, T. P., Generazio, E. R., and Gyekenyesi, J.Z., "Thermal Shock Fiber-Reinforced Ceramic Matrix Composites," *Ceram. Eng. and Sci. Proc.*, 12[7–8], 1500–1508, 1991.
- [126] Kagawa, Y., "Thermal Shock Damage in a Two-Dimensional SiC/SiC Composite Reinforced with Woven SiC Fibers," *Composites Science and Technology*, 57, 607–611, 1997.
- [127] Wang, H., Singh, R. N., and Lowden, R. A., "Thermal Shock Behavior of Unidirectional, 0/90 and 2-D Woven Fiber-Reinforced CVI SiC Matrix Composites," *J. Mater. Sci.*, 32[12], 3305–3313, 1997.
- [128] Guillaumat, L. and Lamon, J., "Multi Fissuration de Composites SiC/SiC," (Multi-cracking of SiC/SiC Composites) in *Microstructure, Comportements Thermomécaniques et Modélisation des Composites Céramique-Céramique à Fibres*, Vol. 3., Chermant, J. L. and Fantozzi, G., eds., Hermès, Paris, France, 1993. pp. 159–172 (in French).
- [129] Gasser, A., Ladeveze, P., and Poss, A., "Damage Mechanisms of a Woven SiC/SiC Composite: Modelling and Identification," *Composites Science and Technology*, 56, 779–784, 1996.
- [130] Guillaumat, L. and Lamon, J., "Model of the Nonlinear Stress-Strain Behavior of a 2D-SiC/SiC Ceramic Matrix Composite (CMC)," *Ceramic Transactions*, 57, 215–220, 1995.
- [131] Akimune, Y., Ogasawara, T., Akiba, T., and Hirosaki, N., "Spherical Particle Impact Damage Behavior of a SiC Fiber-Reinforced Chemical Vapor Infiltrated SiC Composite," *J. Mater. Sci. Letters*, 18, 682–692, 1991.
- [132] Holmes, J. W. and Sorensen, B. F., "Fatigue Behavior of Continuous Fiber-Reinforced Ceramic Matrix Composites," in *High Temperature Mechanical Behavior of Ceramic Composites*, Nair, S. V. and Jakus, K., eds., Butterworth-Heinemann, Newton, MA, USA, 1995. pp. 261–326.
- [133] Reynaud, P., "Cyclic Fatigue of Ceramic-Matrix Composites at Ambient and Elevated Temperatures," *Composites Science and Technology*, 56[7], 809–814, 1996.
- [134] Shuler, S.F., Holmes, JW., Wu, X., and Roach, D., "Influence of Loading Frequency on the Room-Temperature Fatigue of a Carbon-Fiber/SiC-Matrix Composite," *J. Am. Ceram. Soc.*, 76[9], 2327–2336, 1993.
- [135] Lara-Curzio, E., Ferber, M. K., Boisvert R., and Szweda, A., "The High Temperature Tensile Fatigue Behavior of Polymer-derived Ceramic Composites," *Ceram. Eng. and Sci. Proc.*, 16[4], 341–349, 1995.
- [136] Lee, S. S., Zawada, L. P., Staehler, J. M., and Folsom, C. A., "Mechanical Behavior and High-Temperature Performance of a Woven Nicalon/Si-N-C Ceramic-Matrix Composite," *J. Am. Ceram. Soc.*, 81[7], 1797–1811, 1998.
- [137] Steel, S. G., Zawada, L. P., and Mall, S., "Fatigue Behavior of a Nextel 720/Alumina (N720/A) Composite at Room and Elevated Temperature," *Ceram. Eng. and Sci. Proc.*, 22[3], 695–702, 2001.
- [138] Kagawa, Y., Zhu, S., Mizuno, M., and Mutoh, Y., "Monotonic Tension, Fatigue and Creep Behavior of SiC-Fiber-Reinforced SiC-Matrix Composites: A Review," *Composites Science and Technology*, 59[6], 833–851, May 1999.
- [139] Butkus, L. M., Holmes, J. W., Nicholas, T., "Thermomechanical Fatigue Behavior of a Silicon Carbide Fiber-Reinforced Calcium Aluminosilicate Composite," *J. Am. Ceram. Soc.*, 76 [11], 2817–2825, 1993.
- [140] Weinberg, D. J., Myers, F. K., and Holmes, J. W., "Thermal-Mechanical Fatigue of Fiber-Reinforced Ceramics," *Ceram. Eng. and Sci. Proc.* 18[3], 555–569, 1997.
- [141] Evans, A. G., Zok, F. W., McMeeking, R. M., and Du, Z. Z., "Models of High-Temperature, Environmentally Assisted Embrittlement in Ceramic Matrix Composites," *J. Am. Ceram. Soc.*, 79[9], 2345–2352, 1996.

- [142] Jones, R. H., Henager, C. H., and Windisch, C. F., "Stress-Corrosion Cracking of Silicon Carbide Fiber/Silicon Carbide Composites," *J. Am. Ceram. Soc.*, 83[8], 1999–2005, 2000.
- [143] Lara-Curcio E. and Ferber, M. K., "Evolution of Internal Stresses in Composites During Creep," *Ceram. Eng. and Sci. Proc.*, 16[5], 791–800, 1995.
- [144] Holmes, J. W. and Wu, X., "Elevated Temperature Creep Behavior of Continuous Fiber-Reinforced Ceramic Matrix Composites," in *High Temperature Mechanical Behavior of Ceramic Composites*, Nair, S. V. and Jakus, K., eds., Butterworth-Heinemann, Newton, MA, USA, 1995. pp. 261–326.
- [145] Widjaja, S., Jakus, K., Ritter, J. E., Lara-Curcio, E., Sun, E. J., Watkins, T. R., and Brennan, J. J., "Creep-Induced Residual Stress Strengthening in Nicalon™ Fiber-Reinforced BMAS Glass-Ceramic Matrix Composites," *J. Am. Ceram. Soc.*, 82[3], 657–664, 1999.
- [146] Lara-Curcio, E., "Stress-Rupture of Nicalon™/SiC Continuous Fiber Ceramic Composites in Air at 950°C," *J. Am. Ceram. Soc.*, 80[12], 3268–3272, 1997.
- [147] Lara-Curcio, E. and Ferber, M. K., "Stress Rupture of Nicalon™/SiC CFCCs at Intermediate Temperatures," *J. Mater. Sci. Letters*, 16, 23–26, 1997.
- [148] Lara-Curcio, E., "Oxidation-Induced Stress-Rupture of Fiber Bundles," *J. Eng. Mater. and Techn.*, 120, 105–109, April 1998.
- [149] Pysher, D. J., Goretta, K. C., Hodder, R. S., Jr., and Tressler, R.E., "Strengths of Ceramic Fibers at Elevated Temperatures," *J. Am. Ceram. Soc.*, 72[2], 284–288, 1989.
- [150] Lara-Curcio, E., "Analysis of Oxidation-Assisted Stress-Rupture of Continuous Fiber-Reinforced Ceramic Matrix Composites at Intermediate Temperatures," *Composites Part A*, 30[4], 549–554, 1999.
- [151] Verrilli, M. J., Calomino, A. M., and Brewer, D. N., in *Thermal and Mechanical Test Methods and Behavior of Continuous Fiber Ceramic Composites, ASTM STP 1309*, Jenkins, M. G., Gonczy, S. T., Lara-Curcio, E., Ashbaugh, N. E., and Zawada, L. P., eds. American Society for Testing and Materials, 1997. pp. 158–175
- [152] Lipetzky, P., Stoloff, N. S., and Dvorak, G. J., "Atmospheric Effects on High-Temperature Lifetime of Ceramic Composites," *Ceram. Eng. and Sci. Proc.*, 18[4], 355–362, 1997.
- [153] Ogasawara, T., Ishikawa, T., and Suzuki, N., "Tensile Creep Behavior of 3-D Woven Si-Ti-C-O Fiber/SiC-based Matrix Composite with Glass Sealant," *J. Mater. Sci.*, 35, 785–793, 2000.
- [154] Mizuno, M., Zhu, S., Kagawa, Y., and Kaya, H., "Stress, Strain and Elastic Modulus Behavior of SiC/SiC Composites During Creep and Cyclic Fatigue," *J. Eur. Ceram. Soc.*, 18[13], 1869–1878, 1998.
- [155] Kleykamp, H., Schauer, V., and Skokan, A., "Oxidation Behavior of SiC Fiber-reinforced SiC," *Journal of Nuclear Materials*, 227, 130–137, 1995.
- [156] Fox, D. and Nguyen, Q. N., "Oxidation Kinetics of Enhanced SiC/SiC," *Ceram. Eng. and Sci. Proc.*, 16[5], 877–884, 1995.
- [157] De Gaudenzi, G. P., Taut, C., Iffländer, K., and Corcoruto, S., "Environmental Resistance of Ceramic Matrix Composite Materials for Gas Turbine Applications," *Key Engineering Materials*, 132-136[3], 1637–1640, 1997.
- [158] Filipuzzi, L. and Naslain, R., "Oxidation Mechanism and Kinetics of 1D-SiC/C/SiC Composite Materials: II, Modelling," *J. Am. Ceram. Soc.* 77[2], 467–480, 1994.
- [159] Filipuzzi, L., Camus, G., Naslain, R., and Thebault, J., "Oxidation Mechanism and Kinetics of 1D-SiC/C/SiC Composite Materials: I: An Experimental Approach," *J. Am. Ceram. Soc.*, 77[2], 459–466, 1994.

- [160] Lamouroux, F. and Camus, G., "Oxidation Effects on the Mechanical Properties of 2D Woven C/SiC Composites," *J. Eur. Ceram. Soc.*, 14, 177–188, 1994.
- [161] Lamouroux, F., Bertrand, S., Pailler, R., Naslain, R., and Cataldi, M., "Oxidation-Resistant Carbon-Fiber-Reinforced Ceramic-Matrix Composites," *Composites Science and Technology*, 59, 1073–1085, 1999.
- [162] Lamouroux, F., Camus, G., and Thebault, J. "Kinetics and Mechanisms of Oxidation of 2D Woven C/SiC Composites: I, Experimental Approach," *J. Am. Ceram. Soc.*, 77[8], 2049–2057, 1994.
- [163] Ogbuji, L.U., "Degradation of SiC/BN/SiC Composite in the Burner Rig," *Ceram. Eng. and Sci. Proc.*, 19[4], 257–264, 1998.
- [164] Miriyala, N., Kimmel, J., Price, J., More, K. L., Tortorelli, P., Eaton, H., Linsey, G., and Sun, E., "The Evaluation of CFCC Liners After Field Testing in a Gas Turbine," ASME paper GT-2002-30585, presented at the ASME Turbo Expo 2002, Land, Sea & Air, Amsterdam, The Netherlands, June 3–6, 2002.
- [165] Jacobson, N. S., Smialek, J. L., Fox, D. S., and Opila, E. J., "Durability of Silica-Protected Ceramics in Combustion Atmospheres," *Ceram. Trans.*, 57, 157–170, 1995.
- [166] Opila, E. J. and Hann, R. E., "Paralinear Oxidation of CVD SiC in Water Vapor," *J. Am. Ceram. Soc.*, 80[1], 197–205, 1997.
- [167] Opila, E. J., Fox, D. S., and Jacobson, N. S., "Mass Spectrometric Identification of Si-O-H(g) Species from the Reaction of Silica with Water Vapor at Atmospheric Pressure," *J. Am. Ceram. Soc.*, 80[4], 1009–1012, 1997.
- [168] Webster, J.D., Hayes, F.H., and Taylor, R., "Thermodynamic Modeling and Experimental Studies in the Design of Integrated Oxidation Protection Systems for Ceramic Matrix Composites," *Key Engineering Materials*, 127–131[2AB], 1225–1232, 1997.
- [169] Lee, K. N., "Current Status of Environmental Barrier Coatings for Si-Based Ceramics," *Surface and Coatings Technology*, 133–134, 1–7, Nov. 2000.
- [170] Lee, K. N., Jacobson, N. S., and Miller, R. A., "Refractory Oxide Coatings on SiC Ceramics," *MRS Bulletin*, 35–38, October 1994.
- [171] Eaton, H. E. and Linsey, G. D., "Accelerated Oxidation of SiC CMCs by Water Vapor and Protection Via Environmental Barrier Coating Approach," *J. Eur. Ceram. Soc.*, 22[14–15], 2741–2747, 2002.
- [172] Kimmel, J., Miriyala, N., Price, J., More, K., Tortorelli, P., Eaton, H., Linsey, G., and Sun, E., "Evaluation of CFCC Liners with EBC After Field Testing in a Gas Turbine," *J. Eur. Ceram. Soc.*, 22[14–15], 2769–2775, 2002.
- [173] Richardson, G. Y., Kowalik, R. W., "Oxidation and Hot Corrosion of Dupont Lanxide Enhanced SiC/SiC and Hitco SiC/C Composites," *Ceram. Eng. and Sci. Proc.*, 18[3], 599–606, 1997.
- [174] Kumar, A., Oppici, M.A., Fox, A. G., and Wang S., "Effects of Hot Corrosion on the Microstructure of a Silicon Carbide Fiber-Reinforced Calcium Aluminosilicate," *Ceram. Trans.*, 57, 455–458, 1995.
- [175] Lara-Curzio, E., "Continuous Fiber Ceramic Composite Program Task 2: Supporting Technologies," in *Bimonthly Progress Report for December-January 1996*, Oak Ridge National Laboratory, Oak Ridge, TN, USA, 1996. pp. 25–29.
- [176] Sato, K., Tezuka, A., Funayama, O., Isoda, T., Terada, Y., Kato, S., and Iwata, M., "Fabrication and Pressure Testing of a Gas-Turbine Component Manufactured by a Preceramic-Polymer Impregnation Method," *Composites Science and Technology*, 59 853–859, 1999. © 2000, Elsevier, All rights reserved.
- [177] Wilson, D. M., and Visser, L. R., "Nextel 650 Ceramic Oxide Fiber: New Alumina-Based Fiber For High Temperature Composite Reinforcement," *Ceram. Eng. and Sci. Proc.*, 21[4], 363–373, 2000.